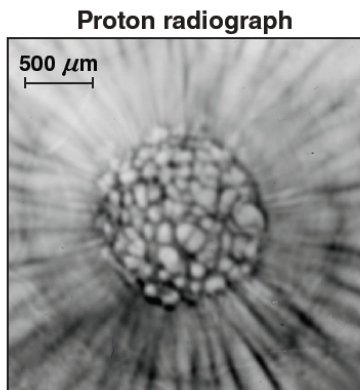


Laser-Driven High-Energy-Density Plasmas and Their Diagnostics

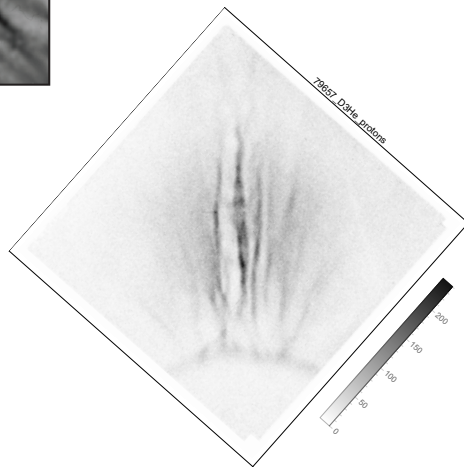


Rayleigh-Taylor Instability

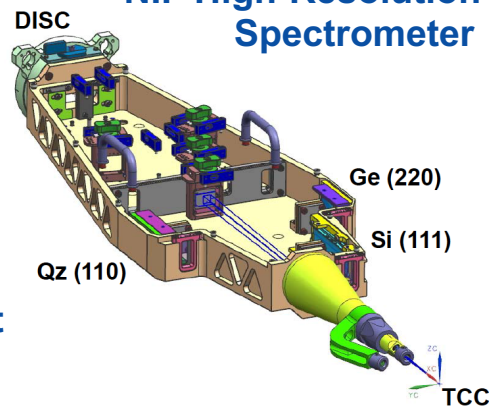


$t = t_0 + 2.6 \text{ ns}$

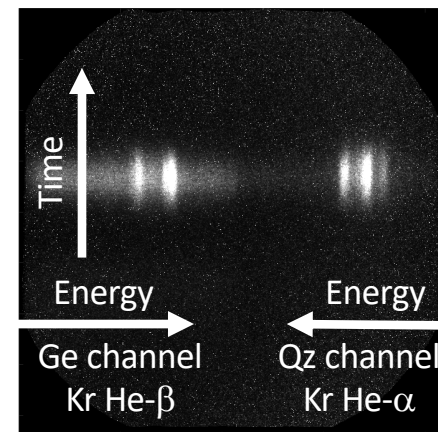
Magnetized Jet



NIF High-Resolution X-ray Spectrometer

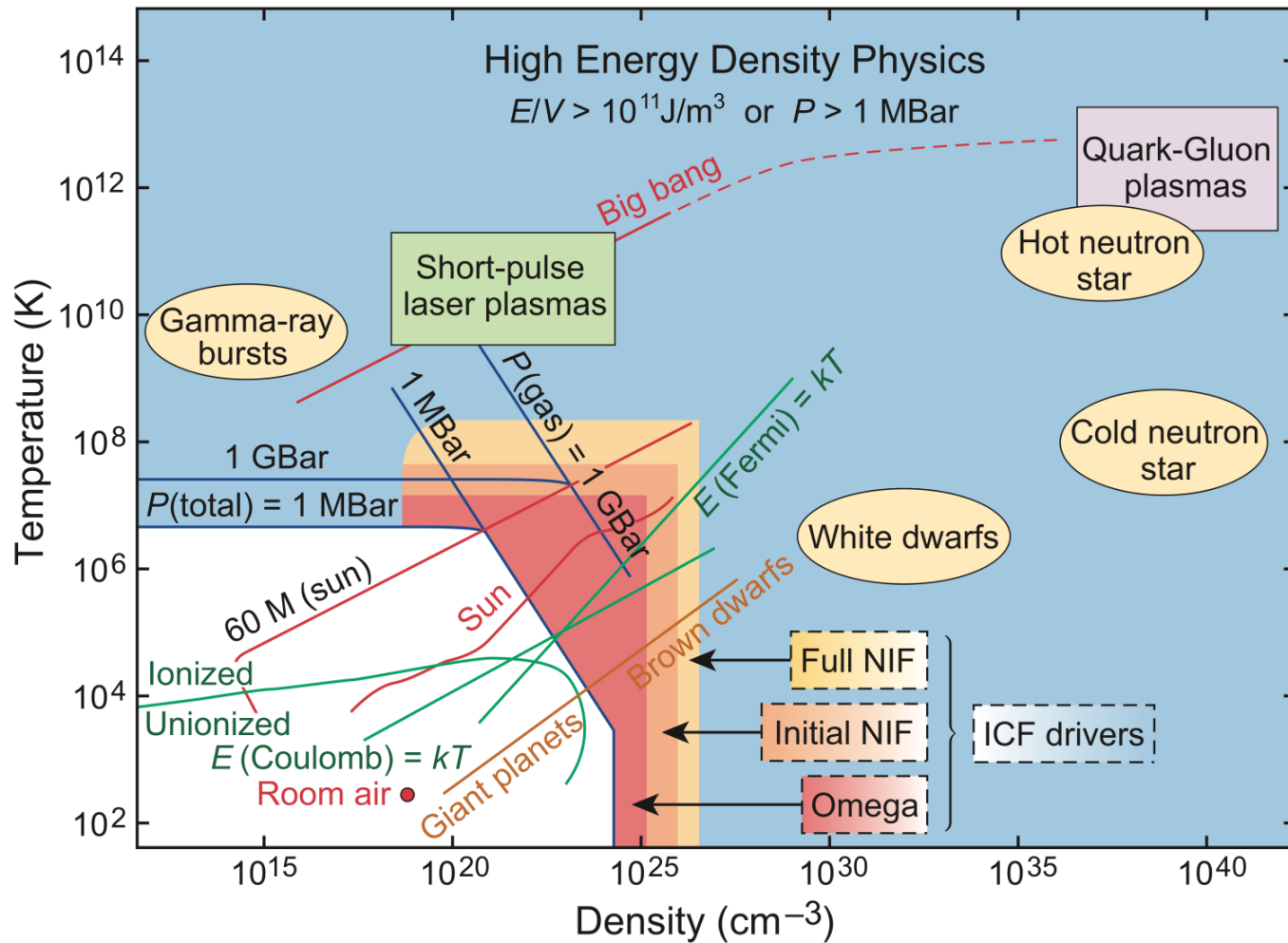


NIF High-Resolution X-ray Spectrometer



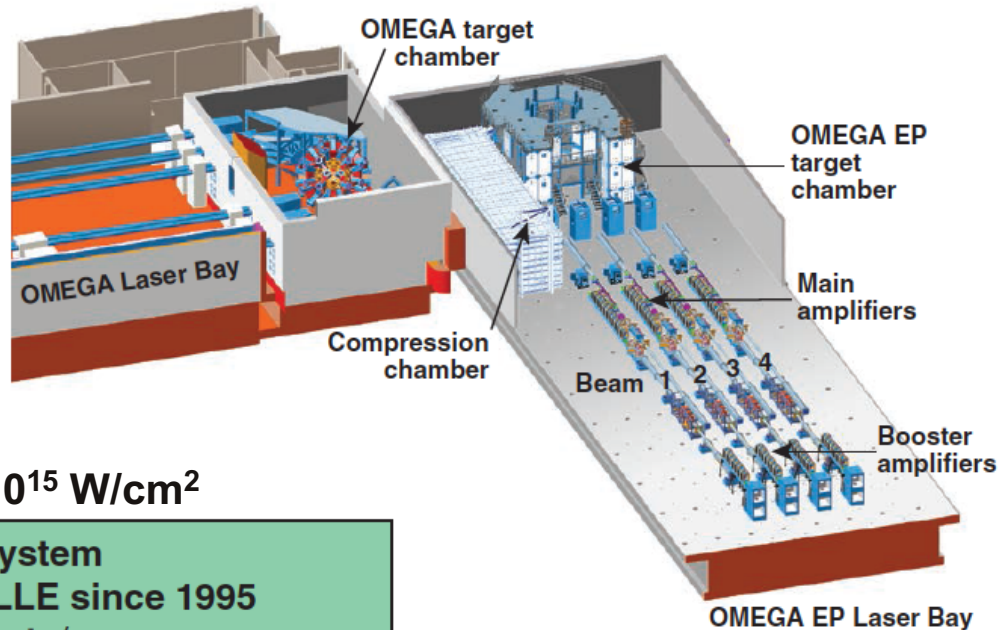
- **Introduction**
 - **High energy density (HED) physics**
 - **Inertial confinement fusion**
 - **Laser-driven HED systems**
 - **Diagnostic requirement**
- **Basic diagnostic building blocks**
 - **Electromagnetic field**
 - **Particles**
 - **X rays**
 - **Pinhole imaging**
 - **Streak cameras**
 - **Framing cameras**
 - **Plasma conditions**

High energy density (HED) physics concerns the study of matter at high densities and extreme temperatures*



* *Frontiers in high energy density physics : The X-games of contemporary science.* (The National Academies Press, Washington, DC, 2003).

Laboratory for laser energetics (LLE) at University of Rochester operates two of the world's large lasers for HED physics research



$$I \sim 10^{14} - 10^{15} \text{ W/cm}^2$$

OMEGA Laser System

- Operating at LLE since 1995
- Up to 1500 shots/year
- Fully instrumented
- 60 beams
- >30-kJ UV on target
- 1% to 2% irradiation nonuniformity
- Flexible pulse shaping
- Short shot cycle (1 h)

More than half of OMEGA's shots are for external users.

$$I \sim 10^{18} \text{ W/cm}^2$$

OMEGA EP Laser System

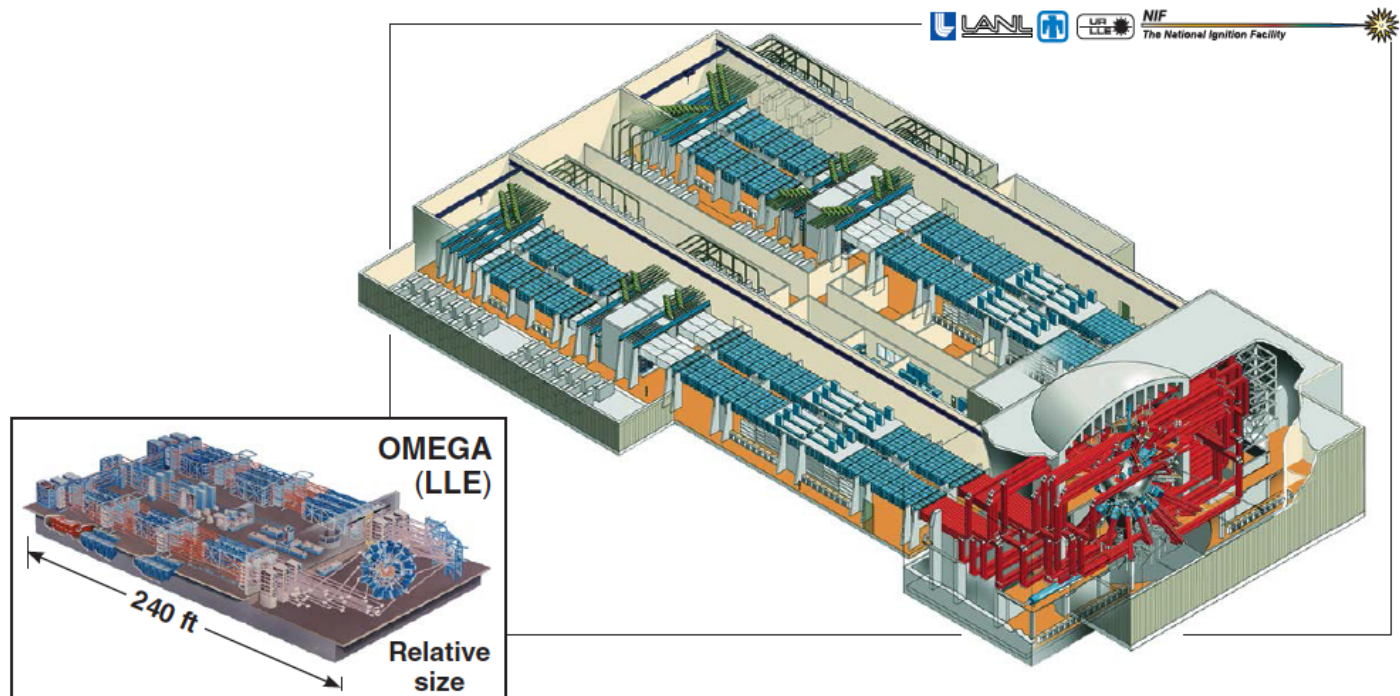
- Completed 25 April 2008
- Four NIF-like beamlines; 6.5-kJ UV (10 ns)
- Two beams can be high-energy petawatt
 - 2.6-kJ IR in 10 ps
 - can propagate to the OMEGA or OMEGA EP target chamber



The National Ignition Facility (NIF) at LLNL aims at demonstrating fusion ignition



- The NIF is a 1.8-MJ laser system (60× OMEGA's energy); NIF is a \$3.5 billion facility completed in 2009
- The NIF is performing experiments with the goal of achieving ignition



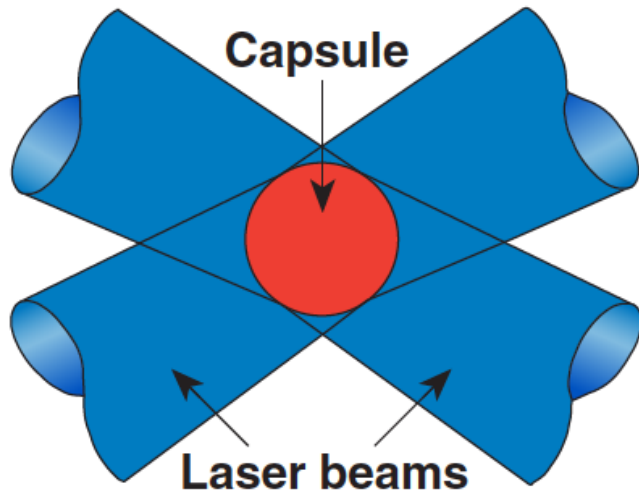
The achievement of ignition—a national “grand challenge”—on the NIF will change the fusion landscape.

* How NIF works, <https://www.youtube.com/watch?v=yixhyPN0r3g>

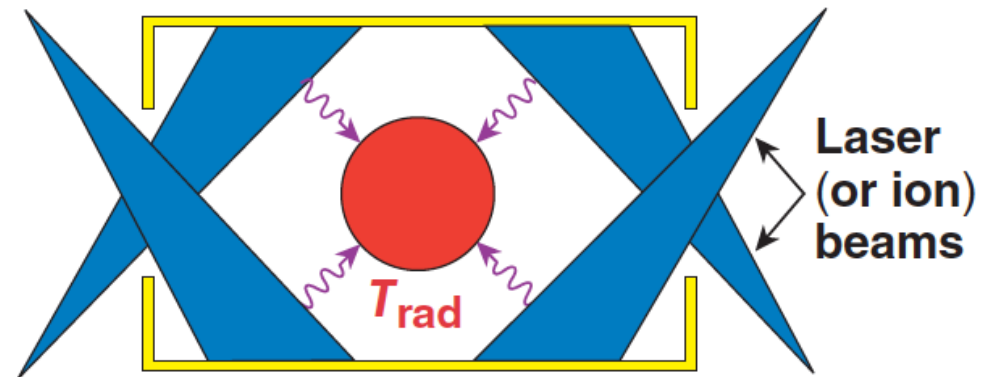
Both direct and indirect (x-ray) drive are being used to implode the inertial confinement fusion capsules



Direct-drive target



X-ray-drive target



Hohlraum using
a cylindrical high-Z case
 T_{rad} is the x-ray temperature

Key physics issues

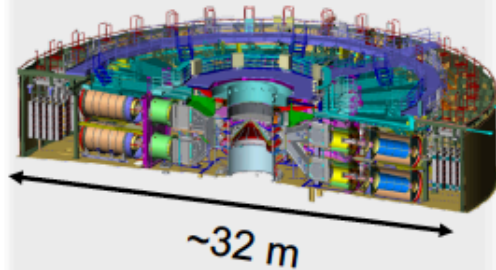
- Energy coupling
- Drive uniformity
- Hydrodynamic instabilities
- Compressibility



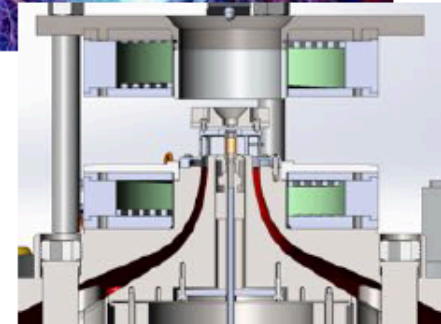
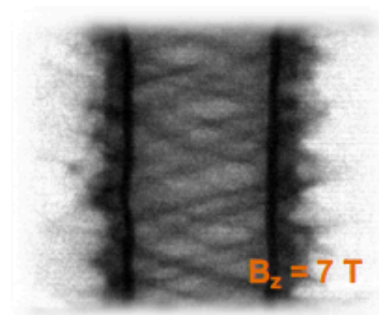
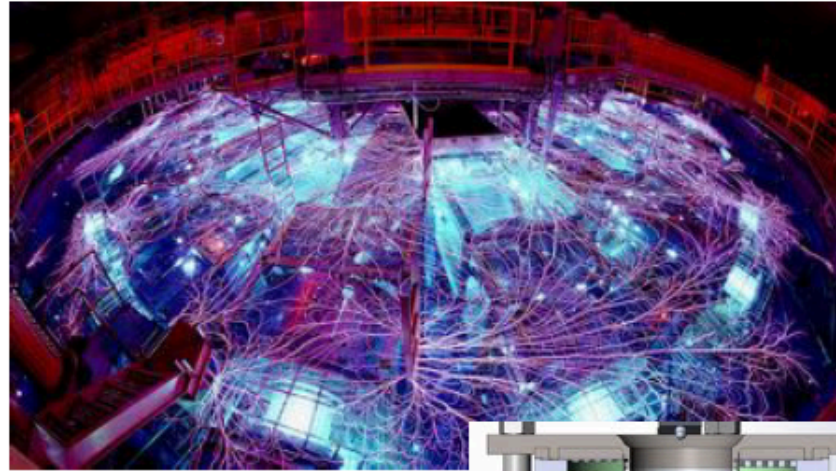
Magnetic drive ICF is being pursued at the Z pulsed power facility at Sandia National Laboratories, NM



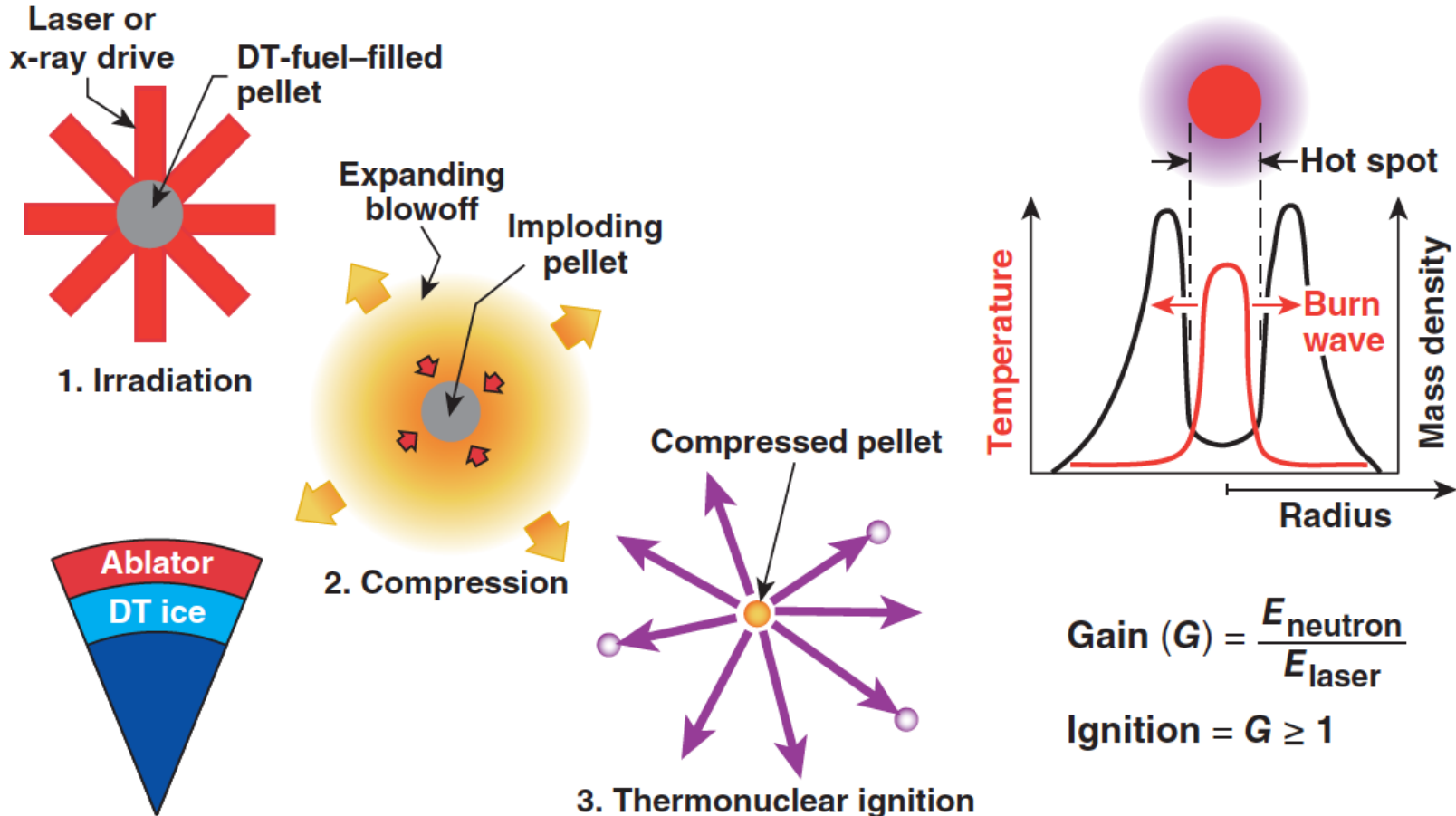
Z Facility



- 80 TW peak electrical power
- Up to ~1 MJ of electrical energy
- Optimized for magnetic drive



Ablation is used to generate the extreme pressures required to compress a fusion capsule to ignition



“Hot-spot” ignition requires the core temperature to be at least 5 keV and the core fuel areal density to exceed $\sim 300 \text{ mg/cm}^2$.



Intense lasers create HED conditions in the laboratory through ablation



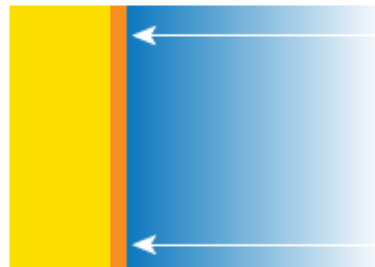
Initial target



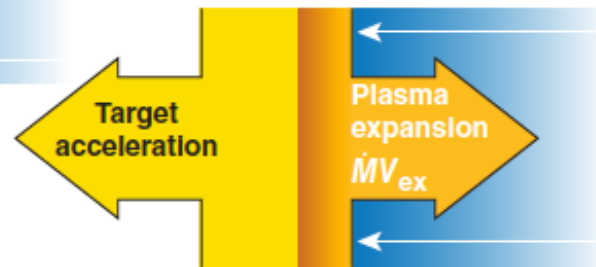
$$P_{\text{abl}}^* (\text{Mbar}) = 40 \left[\frac{I(10^{15} \text{ W/cm}^2)}{\lambda(\mu\text{m})} \right]^{2/3}$$

at $I = 10^{15}$, $\lambda = 0.35 \mu\text{m}$, $P_{\text{abl}} = 80 \text{ Mbar}$

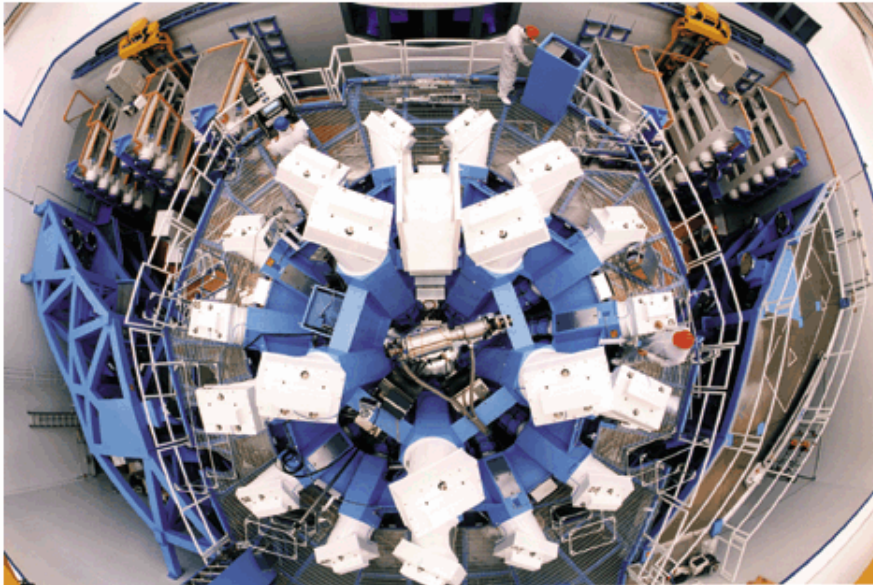
The target surface is heated



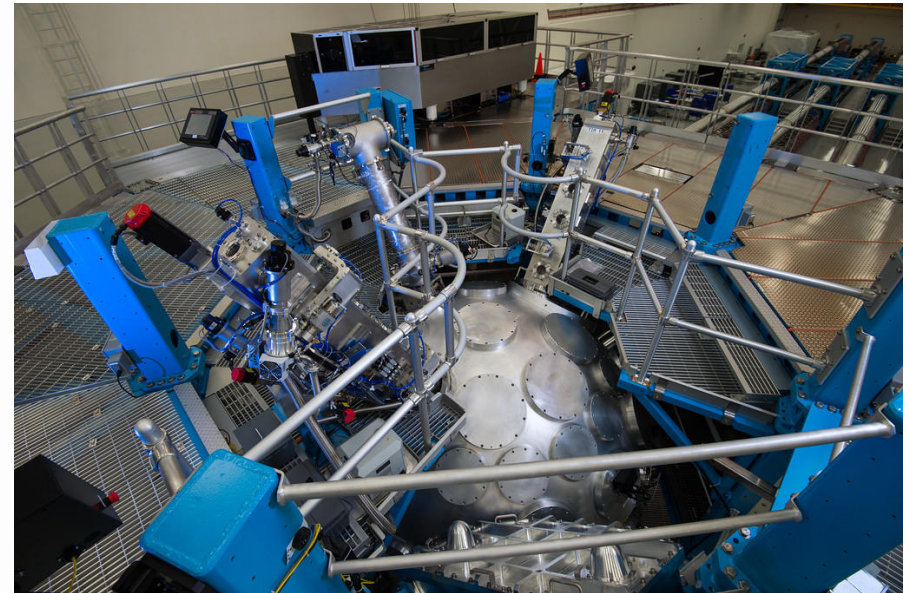
The plasma expands off the front surface, applying pressure to the target



If you look at the OMEGA target chamber



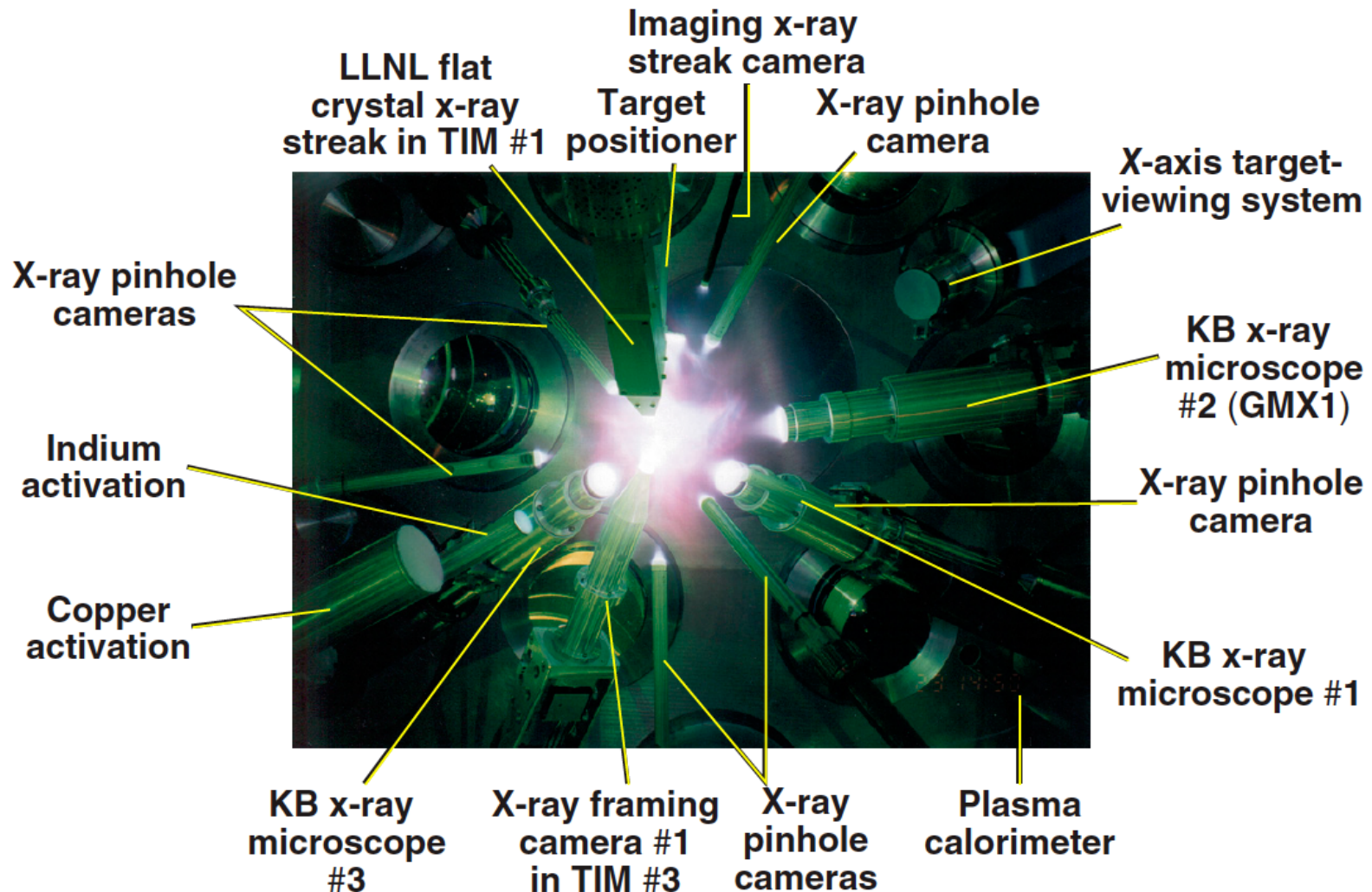
OMEGA



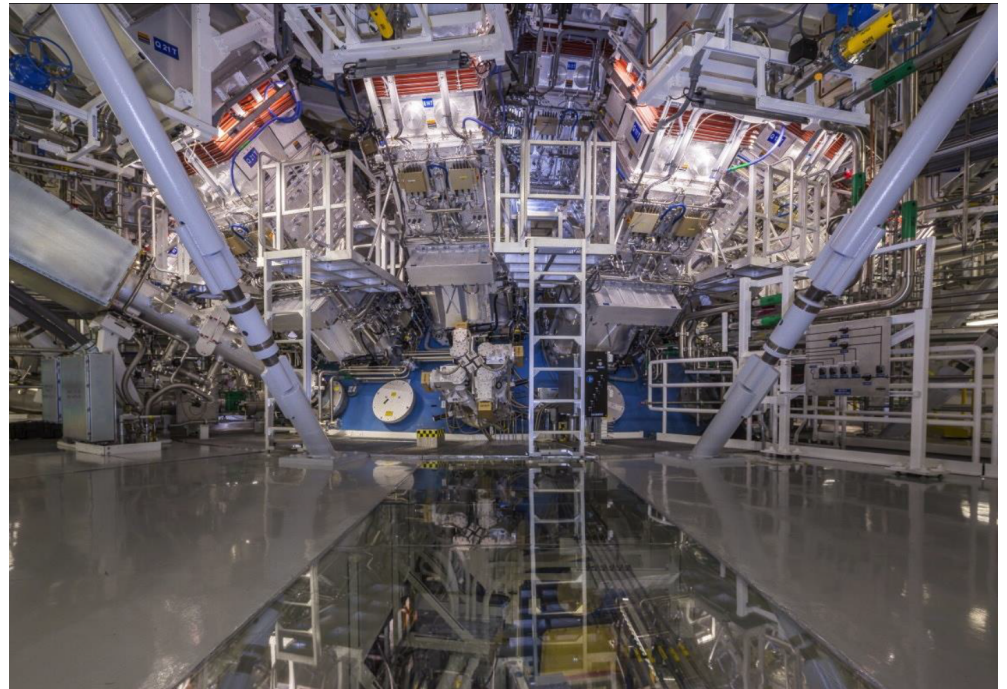
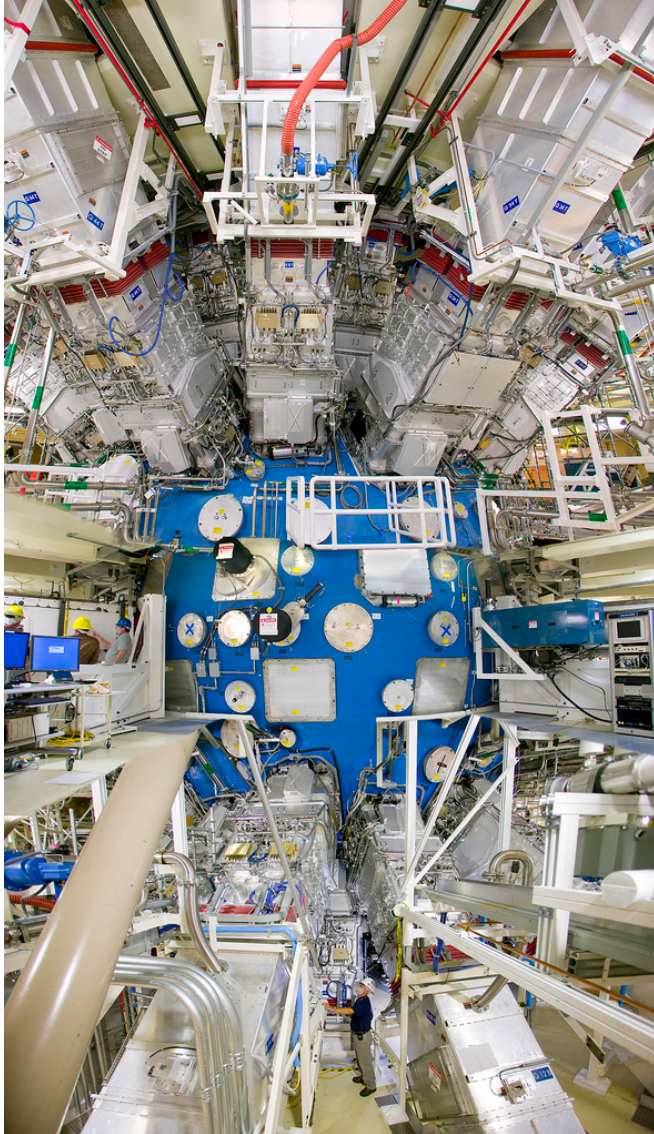
OMEGA EP



If you look at the OMEGA target chamber



The NIF target chamber



The NIF target chamber



Courtesy of Scott Chambliss, Paramount Pictures and Bad Robot Productions.

High-energy-density-physics (HEDP) systems are diagnosed by optical, x-ray, particle and nuclear means



- **HEDP systems generate some or all of**
 - **Visible light**
 - **UV and x-ray photons**
 - **Charged particles**
 - **Neutrons**
 - **Strong fields**
- **A comprehensive diagnostic suite makes it possible to learn a great deal about the systems: field strength and their impact, plasma parameters (n_e , n_i , T_e , v), particles, instabilities, yield, etc...**
- **Diagnosing HED systems require very high temporal (sub-ns, ps) and spatial ($\sim 10\ \mu\text{m}$) resolution**

Diagnostic performance is determined by the resolution and signal-to-noise levels



- Spatial, temporal, or energy resolution determines the diagnostic properties
- The resolution depends on the design and on the signal-to-noise (background) ratio
- The signal level depends on
 - Source brightness
 - Solid angle of the detector $\Delta\Omega = A_{\text{det}}/4\pi D^2$, where A is the effective diagnostic area, and D is the distance from the source to the diagnostic
- The noise (background) level is determined by design and intrinsic noise level (e.g., photon statistics)
- For example, when low number of particles (N) are detected, the uncertainty scales as \sqrt{N}/N

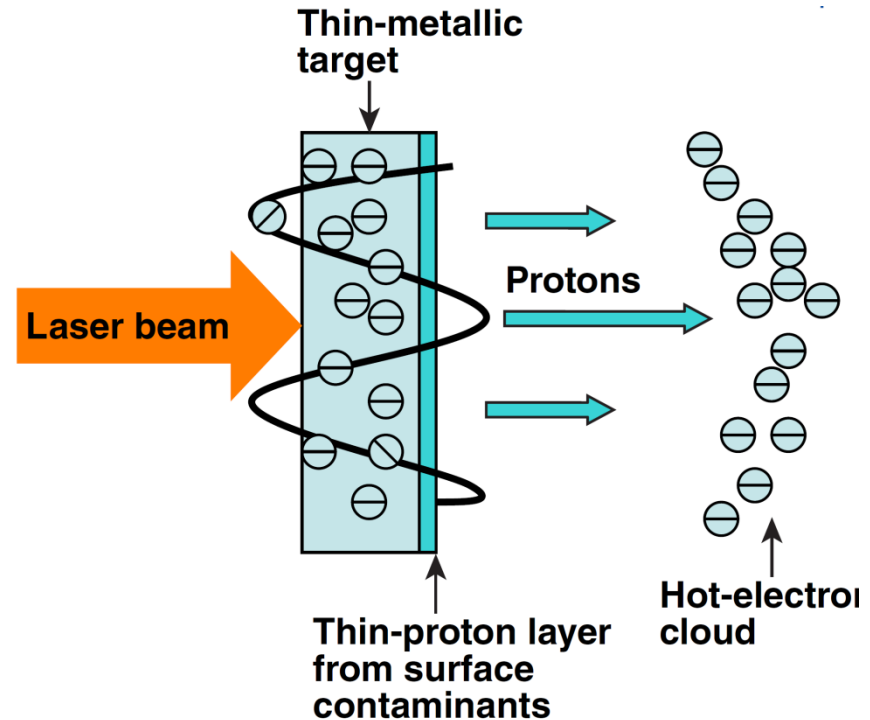
- **Basic diagnostic building blocks**
 - **Electromagnetic field**
 - **Proton radiography**
 - **Particles**
 - **RCF stack / Proton activation pack / Electron spectrometer / Thomson parabola**
 - **X rays**
 - **Pinhole camera (time integrated) / 1-D streak camera / 2-D framing camera**
 - **Plasma conditions**
 - **High-resolution x-ray spectroscopy / Thomson scattering / Neutrons / x-ray radiography**

- **Basic diagnostic building blocks**
 - **Electromagnetic field**
 - **Proton radiography**
 - **Particles**
 - **RCF stack / Proton activation pack / Electron spectrometer / Thomson parabola**
 - **X rays**
 - **Pinhole camera (time integrated) / 1-D streak camera / 2-D framing camera**
 - **Plasma conditions**
 - **High-resolution x-ray spectroscopy / Thomson scattering / Neutrons / x-ray radiography**

Target Normal Sheath Acceleration (TNSA)* generates MeV proton beams in intense ($>10^{18}$ W/cm²) laser-solid interactions



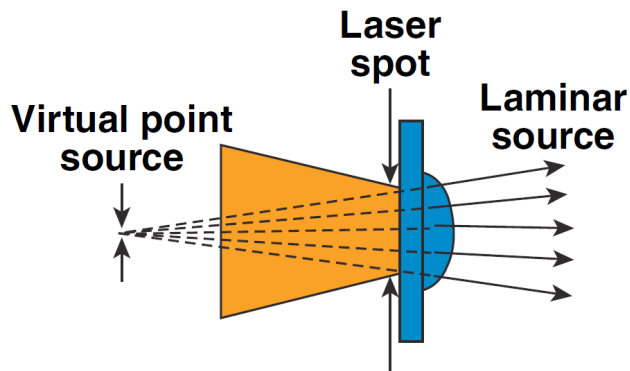
- Hot electrons escape from the rear side of the target
- An electrostatic field is built up, with a field gradient of the order of MeV/ μ m
- Protons are accelerated to tens of MeV



Laser-driven protons are ultra bright, extremely collimated, and have high peak energy (58 MeV) and short burst duration (picosecond scale).

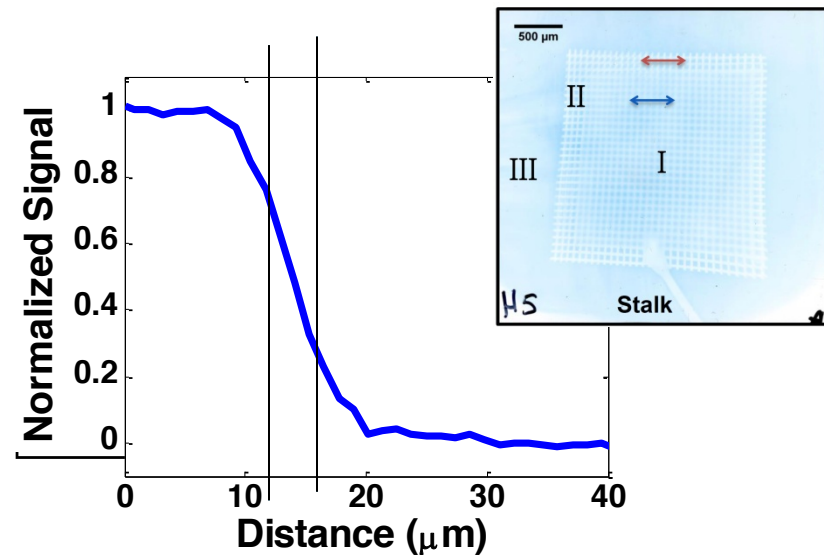
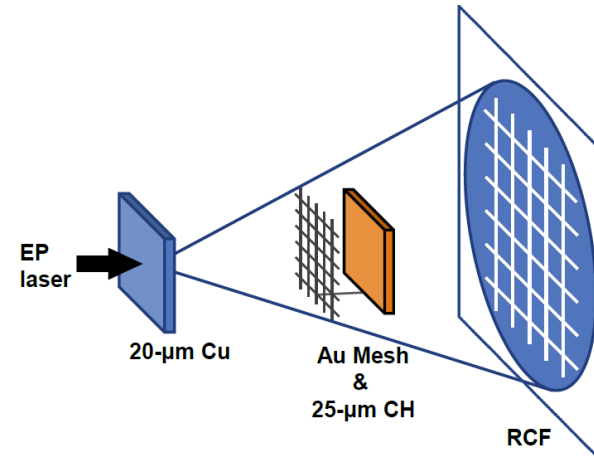
*S. C. Wilks *et al.*, Phys. Plasma 8, 542 (2001)

The virtual proton source is much smaller than the laser spot*



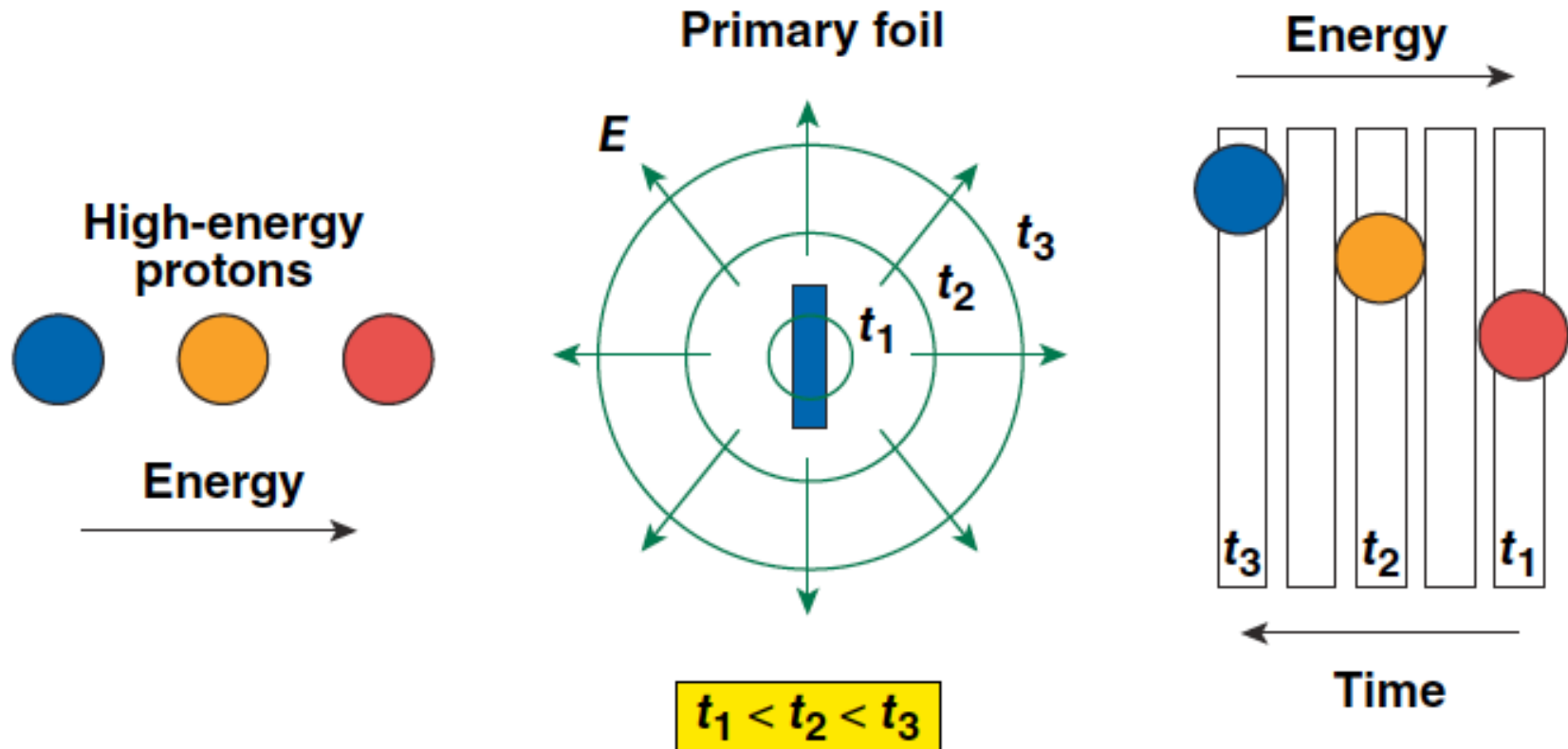
Virtual source size: $4 \pm 2 \mu\text{m}$

Very high spatial resolution!

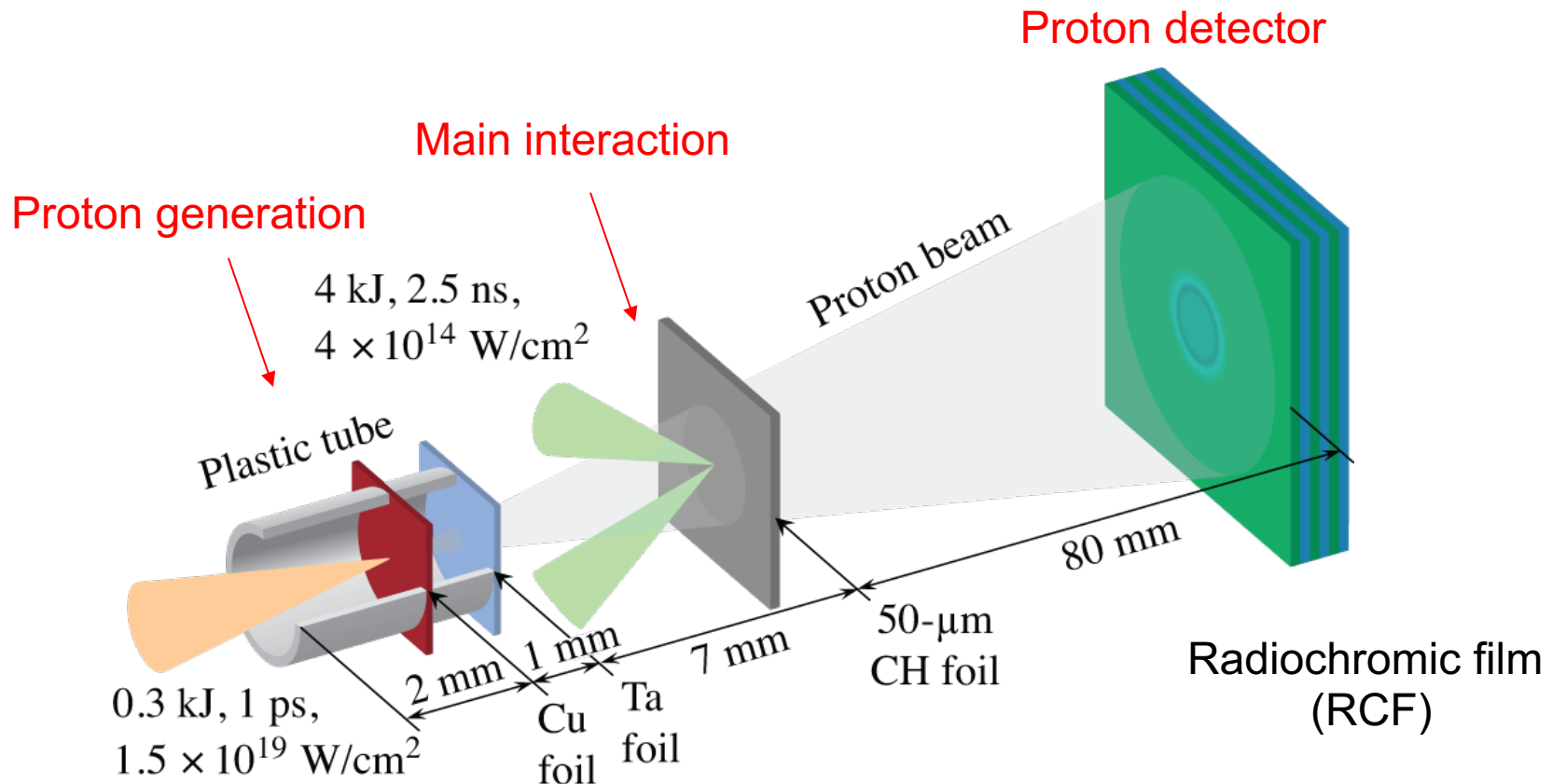


$\sim 8 \mu\text{m}$ for 15 MeV protons

Time-of-flight dispersion and a filtered stack detector produces a multiframe imaging capability



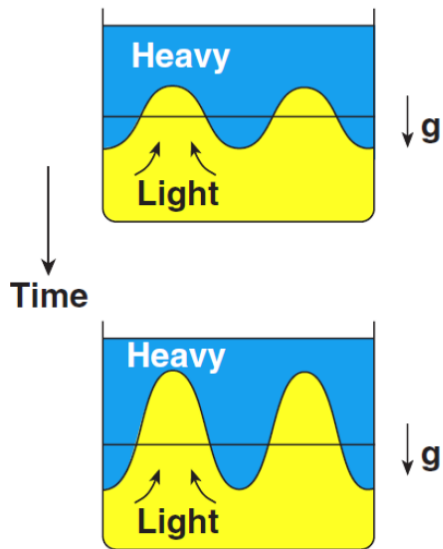
Ultrafast laser-driven proton radiography is developed on OMEGA EP



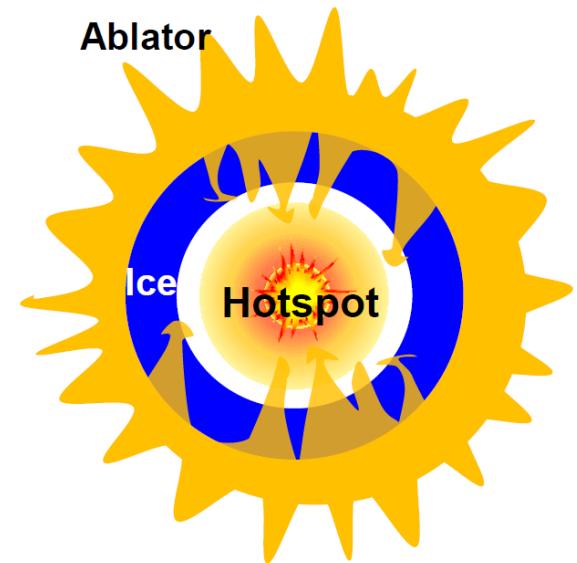
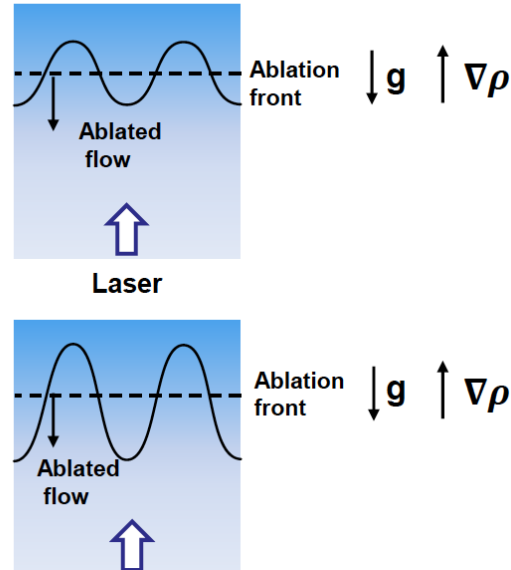
The laser-driven target is subjected to the Rayleigh-Taylor (RT) instability



Classical



Laser-driven target



The RT instability has linear and nonlinear stages*



- Linear regime (classical)**:

$$\eta = \eta_0 e^{\gamma t}$$

$$\gamma = \sqrt{AKg}, \quad A = \frac{\rho_h - \rho_l}{\rho_h + \rho_l}$$

- Linear regime (ablative)**:

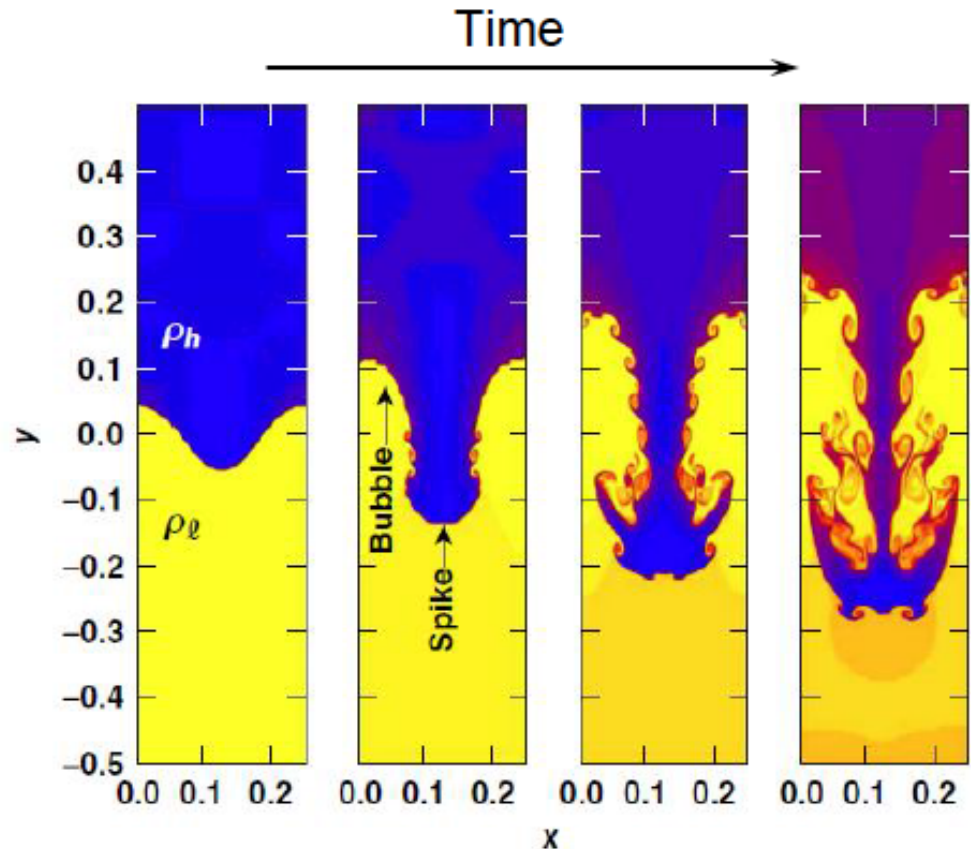
$$\gamma = \alpha \sqrt{\frac{Kg}{1 + \epsilon KL}} - \beta KV_a$$

- Nonlinear regime***: $\eta \geq 0.1\lambda$

Slower growth

Bubbles and spikes

Bubble competition and merger

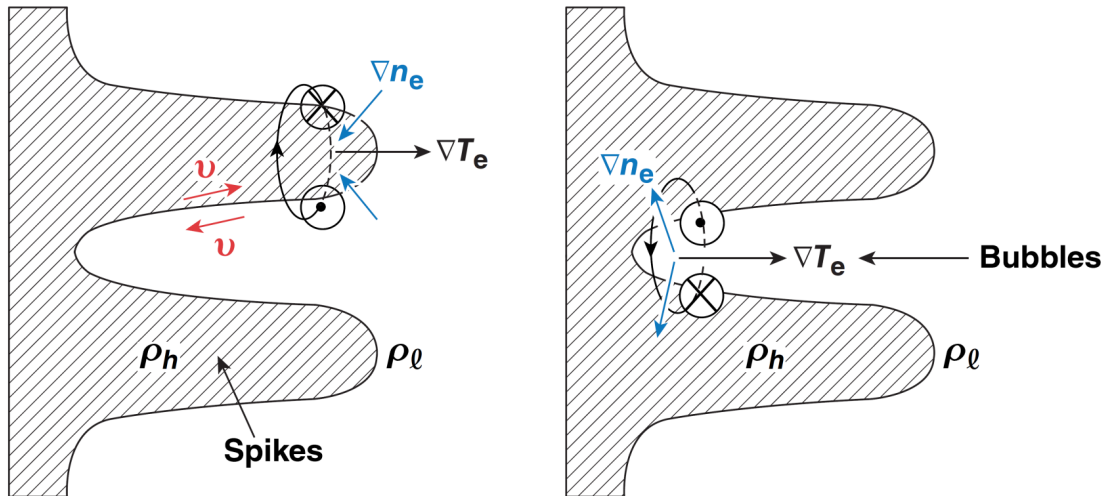


*Shengtai Li and Hui Li. "Parallel AMR Code for Compressible MHD or HD Equations". Los Alamos National Laboratory (2006).

**J. D. Kilkenney et al., Phys. Plasmas 1, 1379 (1994).

*** R. Betti and J. Sanz, Phy. Rev. Lett. 97, 205002 (2006).

Magnetic fields are generated by the Biermann battery mechanism



- Biermann battery:

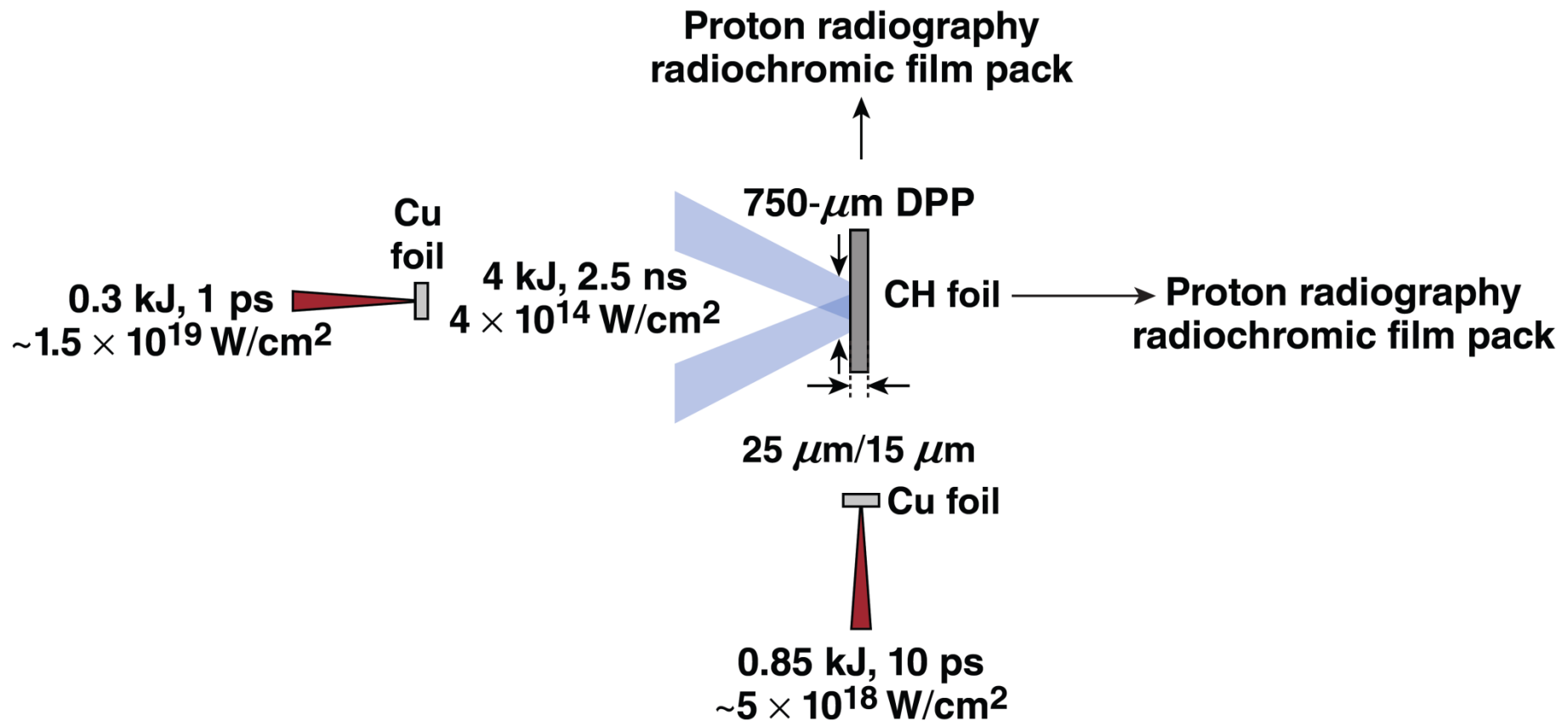
$$\mathbf{E} = -\frac{\nabla P_e}{en_e}$$

$$\frac{\partial \mathbf{B}}{\partial t} = -\nabla \times \mathbf{E} \sim -\frac{\nabla n_e \times \nabla T_e}{en_e}$$

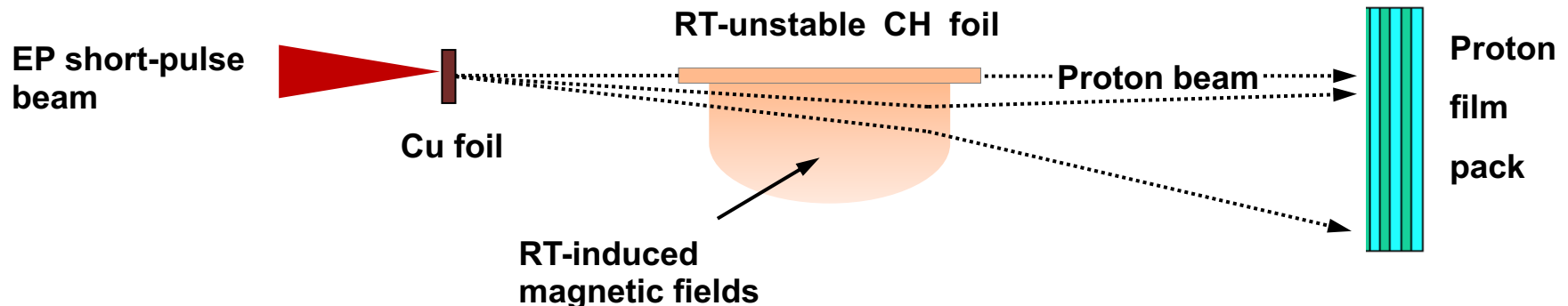
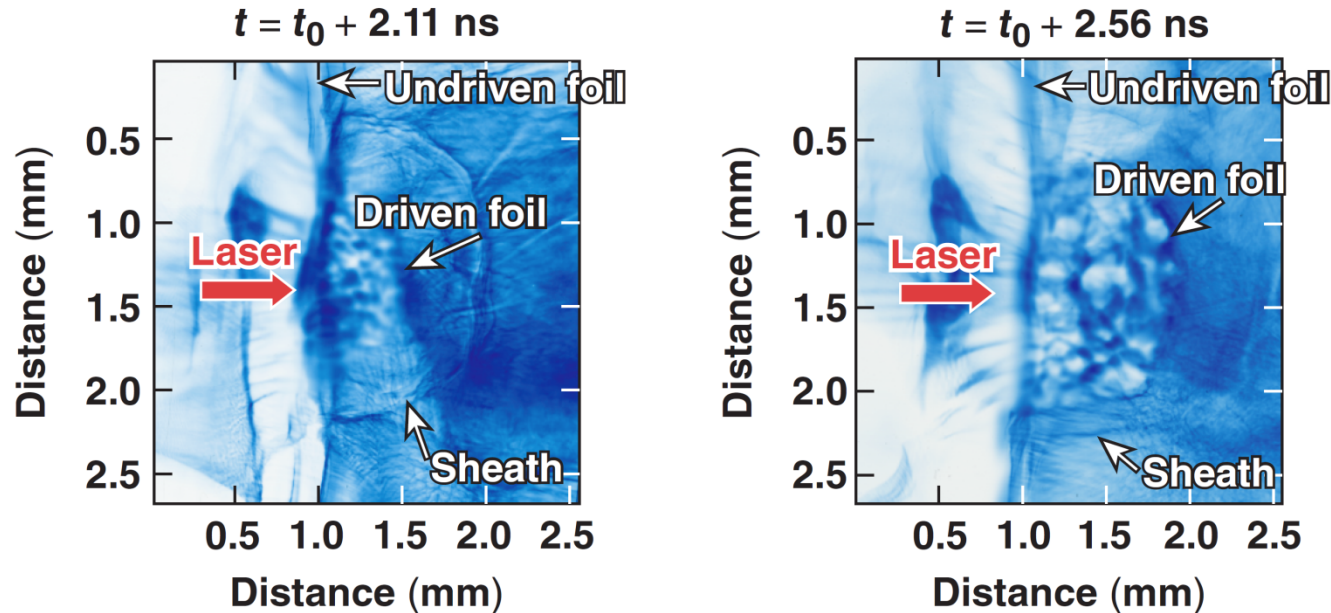
Azimuthal magnetic fields are generated by $\nabla n_e \times \nabla T_e$.

*K. Mima *et al.*, Phys. Rev. Lett., 41, 1715 (1978);
 R. G. Evans, Plasma Phys. Control. Fusion., 28, 1021 (1986);
 B. Srinivasan *et al.*, Phys. Rev. Lett., 108, 165002 (2012).
 M. Manuel *et al.*, Phys. Rev. Lett., 108, 255006 (2012).

Magnetic-field generation has been studied in side-on and face-on geometries using the acceleration of planar plastic targets

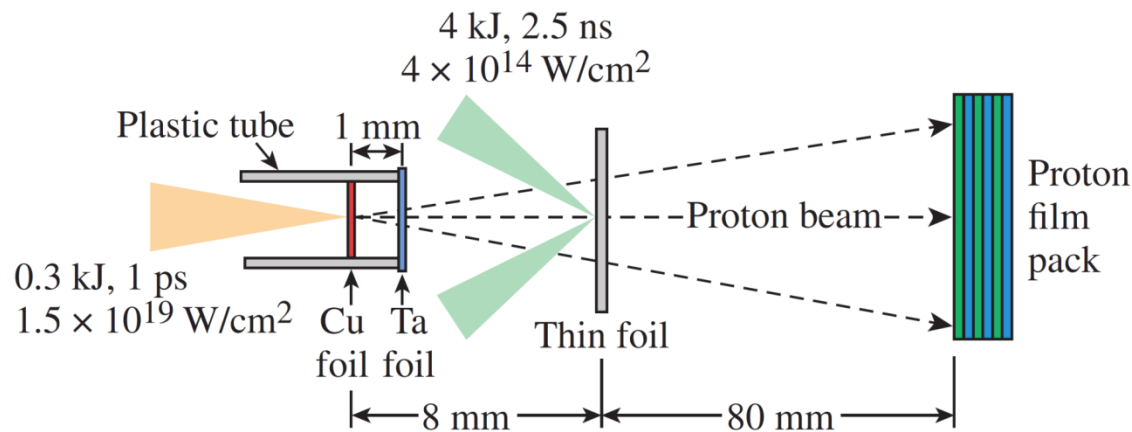


Proton radiography of 15- μm -thick foils reveals magnetic field generation and its evolution*

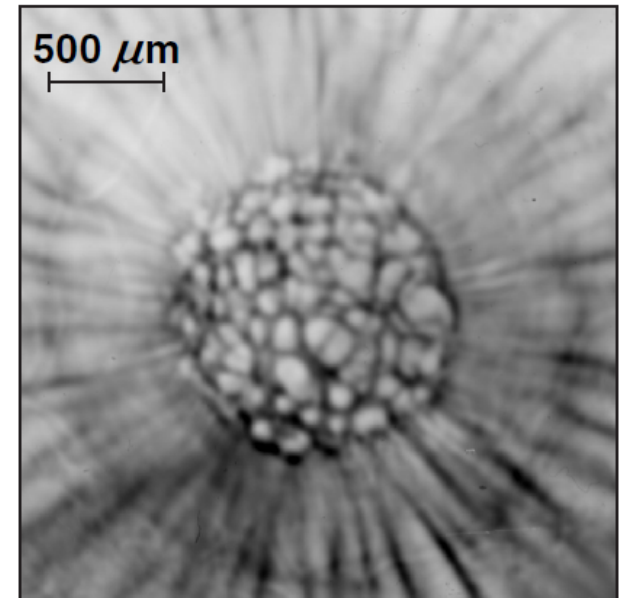


*L. Gao et al., Phys. Rev. Lett. 109, 115001 (2012).

Face-on probing reveals magnetic field generation by the RT instability

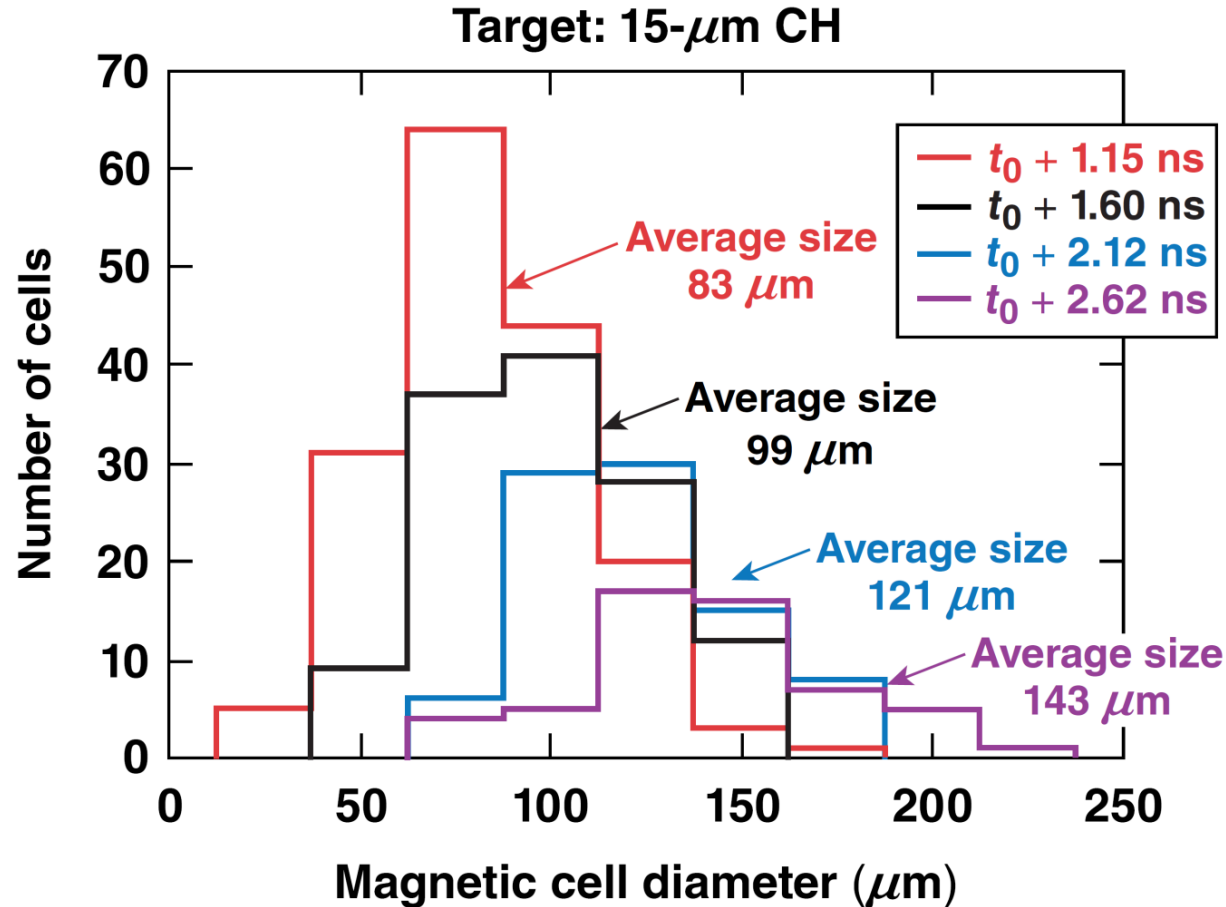


Proton radiograph

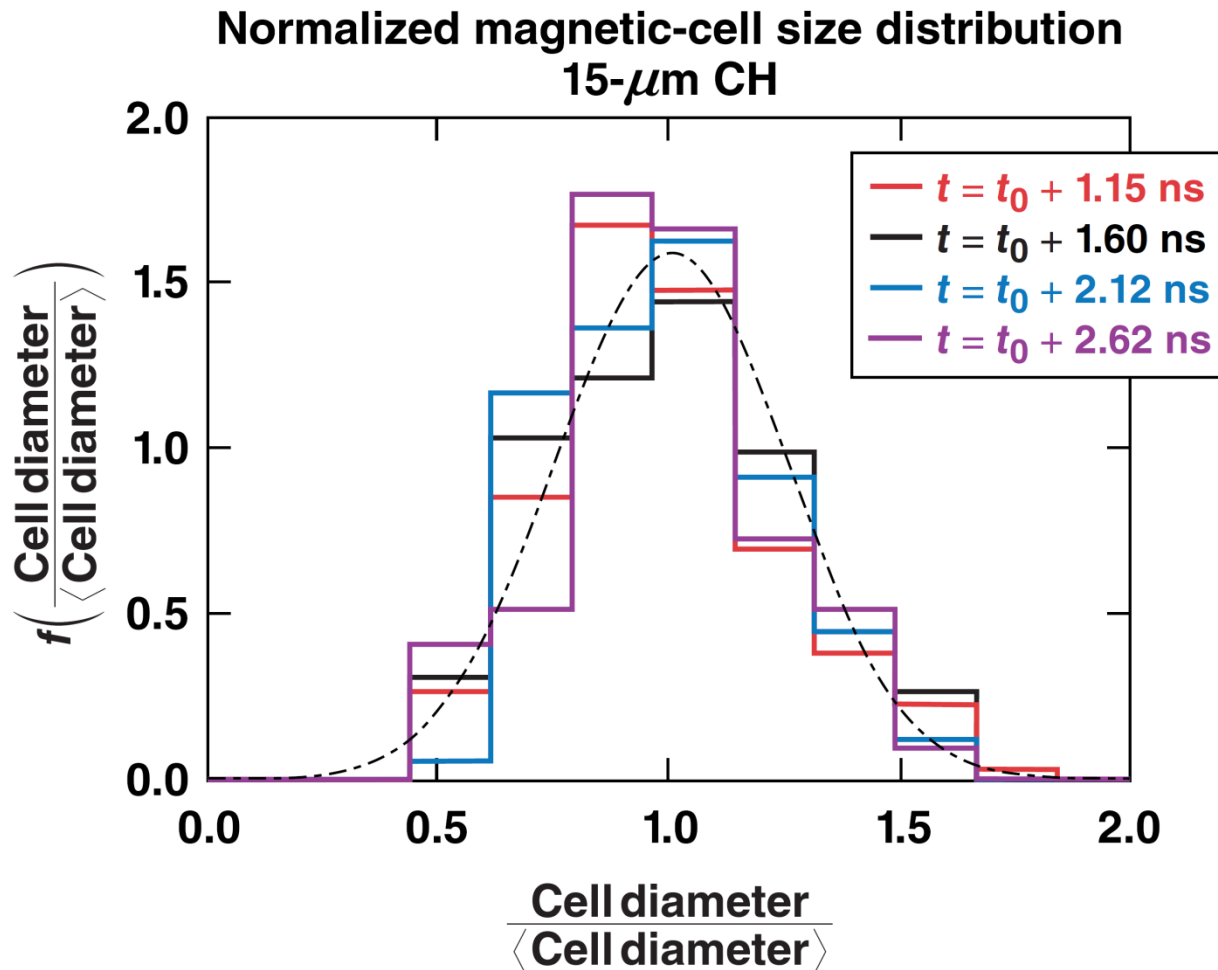


$$t = t_0 + 2.6 \text{ ns}$$

The number of magnetic cells decreases and the magnetic cell diameter increases with time



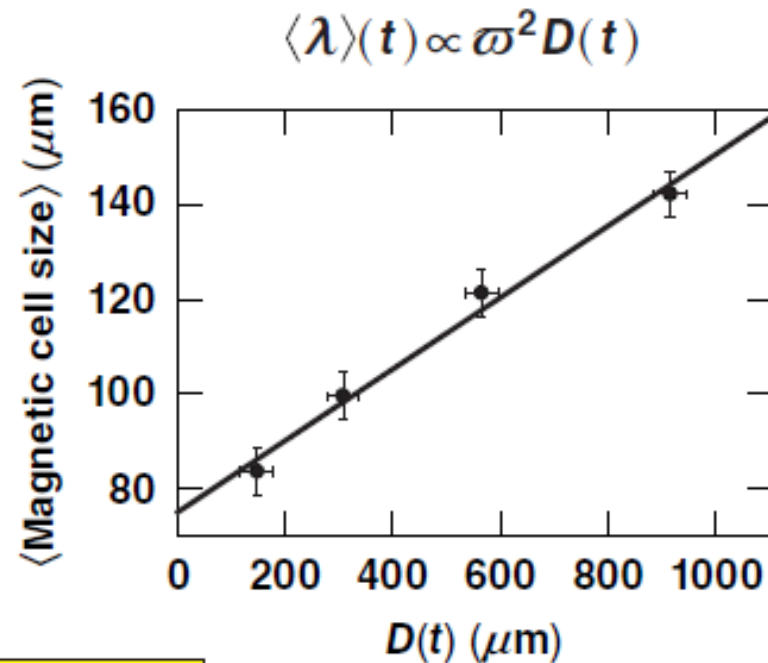
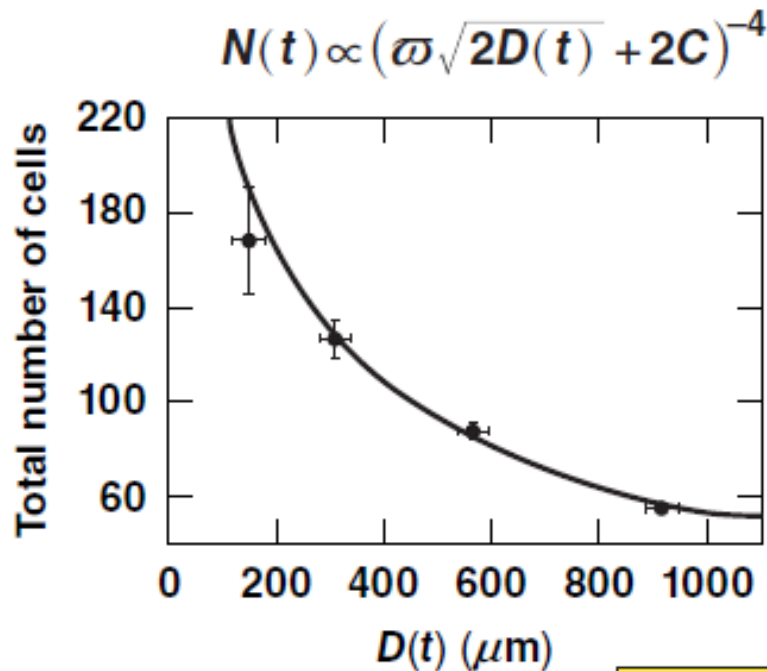
The normalized magnetic-field spatial distribution evolves self-similarly



The evolution of the magnetic-field spatial distribution is consistent with an RT bubble competition and merger model*



Target: 15 μm CH



$$\varpi_{\text{CH}} = 0.79 \pm 0.06^{**}$$

*O. Sadot et al., Phys. Rev. Lett. **95**, 265001 (2005);
D. Oron et al., Phys. Plasmas **8**, 2883 (2001);
U. Alon et al., Phys. Rev. Lett. **72**, 2867 (1994).

L. Gao et al., Phys. Rev. Lett. **110, 185003 (2013).

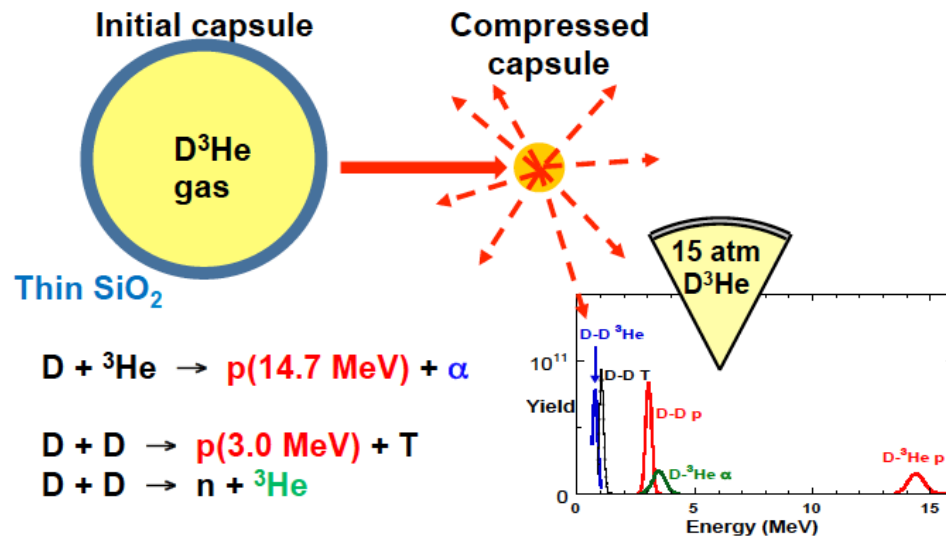
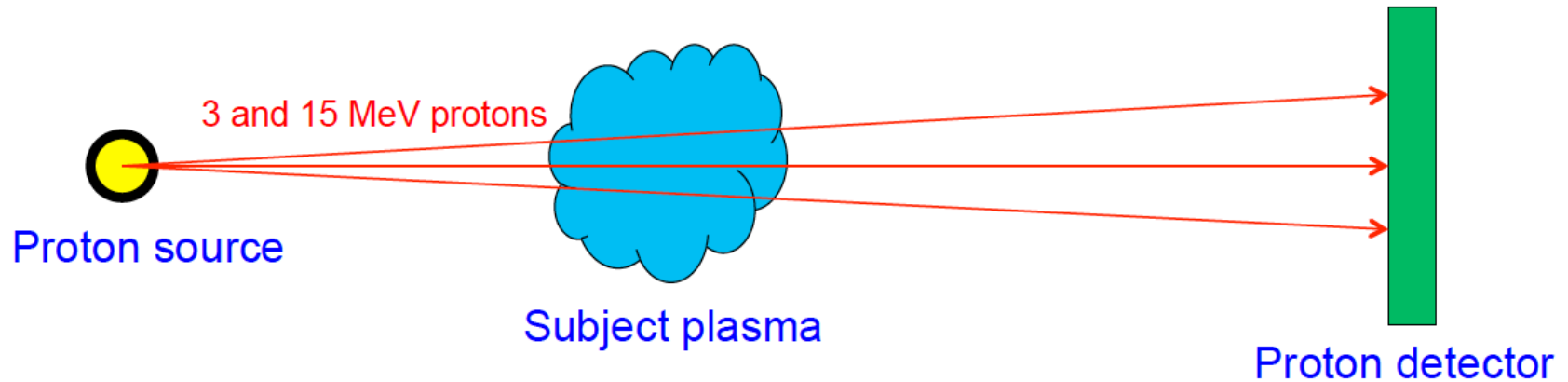
The origin and amplification of the magnetic field in the universe is a central astrophysical problem



- Sources of magnetic fields
- Amplification by the dynamo process
- Flow-dominated systems are common in astrophysics
- Particle acceleration, non-thermal emission



A D³He mono-energetic proton radiography platform has been developed by MIT for HEDP experiments



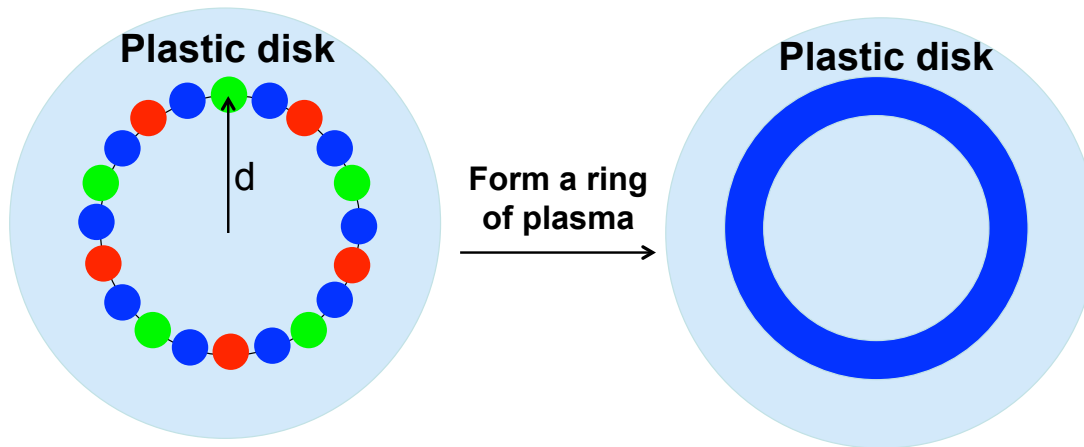
Spatial resolution: ~ 40 μm (FWHM)
Energy resolution: ~ 3%
Temporal resolution: ~ 80 ps

C. K. Li *et al.*, *Phys. Rev. Lett.* (2006)
C. K. Li *et al.*, *Rev. Sci. Instrum.* (2006)
F. Seguin *et al.*, *Rev. Sci. Instrum.* (2003)

A strong, fast propagating, magnetized jet has been created at the OMEGA Laser Facility



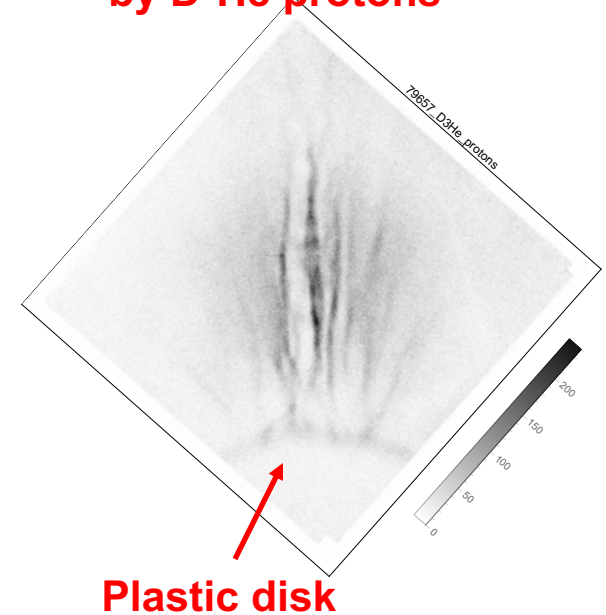
OMEGA Experiment



- P1 axis, Ring 1, 5 beams
- P1 axis, Ring 2, 5 beams
- P1 axis, Ring 3, 10 beams

$d = 0, 400 \text{ um}, \text{ and } 800 \text{ um}$

Magnetized Jet measured by D^3He protons

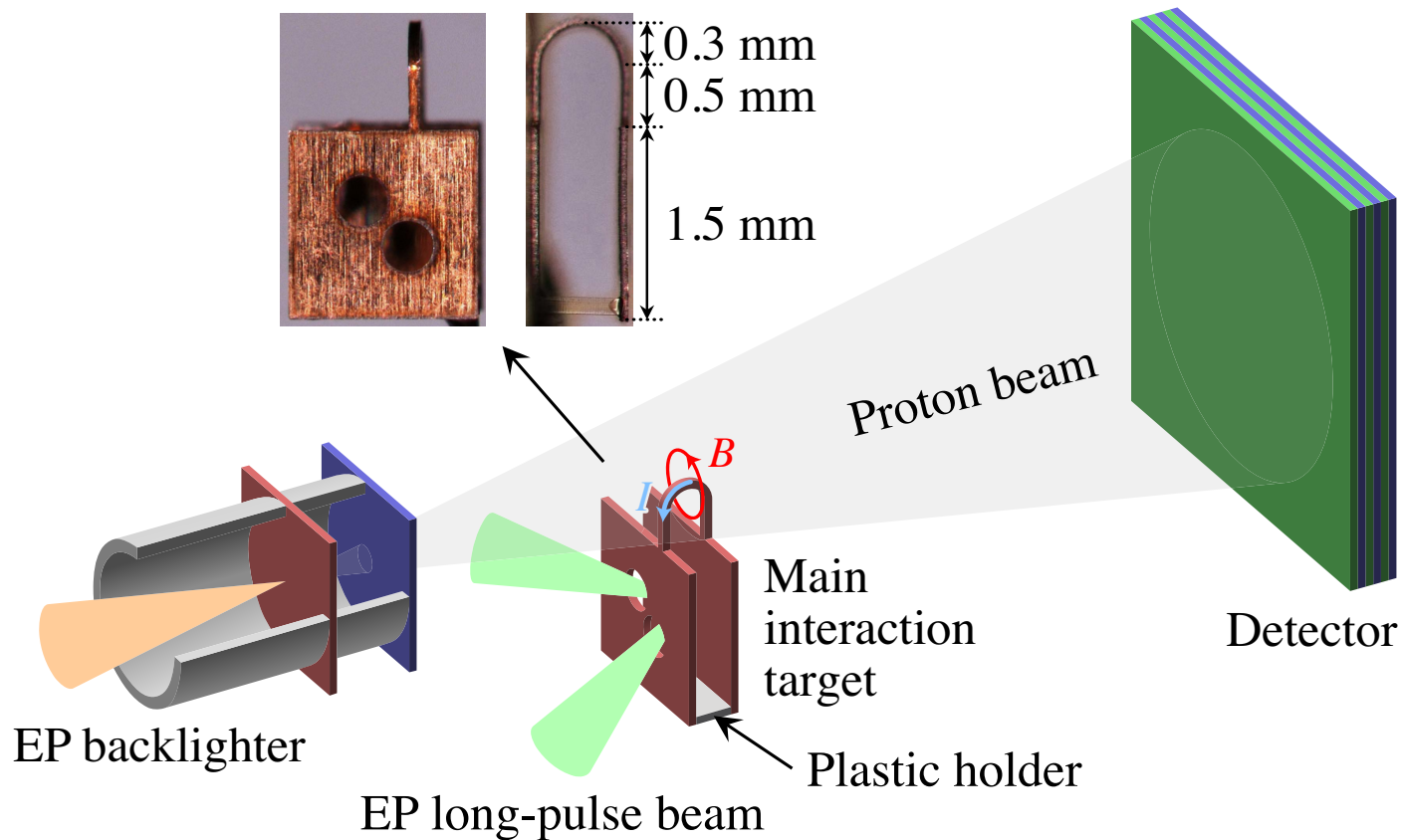


- Collisionless shocks are believed to sites for cosmic ray acceleration
- A magnetized, supersonic jet has been successfully demonstrated*
- The next goal is to collide the jets for collisionless shock

*L. Gao et al., The Astrophysical Journal Letters, 873:L11, 2019



Ultrafast proton radiography directly measured 100s of Tesla magnetic fields generated by a laser-driven capacitor coil target



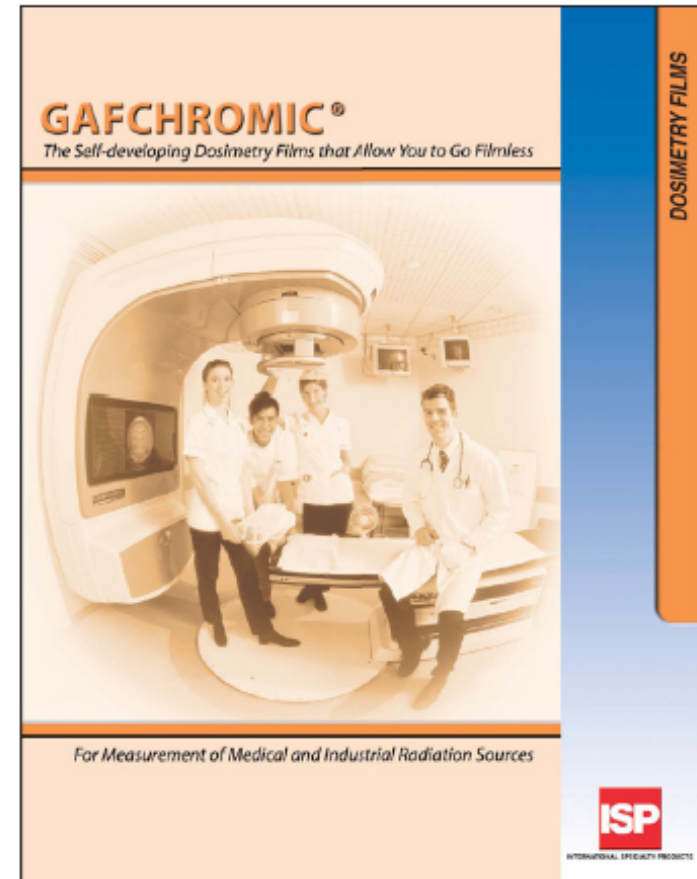
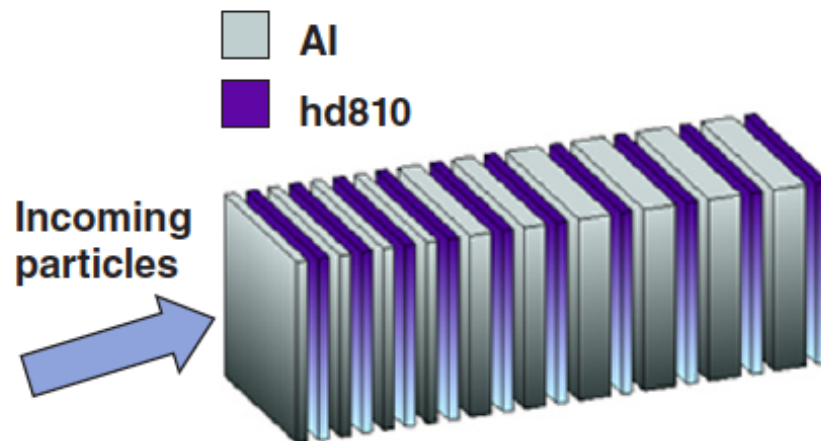
- **Basic diagnostic building blocks**
 - **Electromagnetic field**
 - **Proton radiography**
 - **Particles**
 - **RCF stack / Proton activation pack / Electron spectrometer / Thomson parabola**
 - **X rays**
 - **Pinhole camera (time integrated) / 1-D streak camera / 2-D framing camera**
 - **Plasma conditions**
 - **High-resolution x-ray spectroscopy / Thomson scattering / Neutrons / x-ray radiography**



Radiochromic film allows simple detection of high-energy photons and particles



- Radiochromic film is self-developing and insensitive to visible light
- Multiple layers of film and filters allow energy discrimination

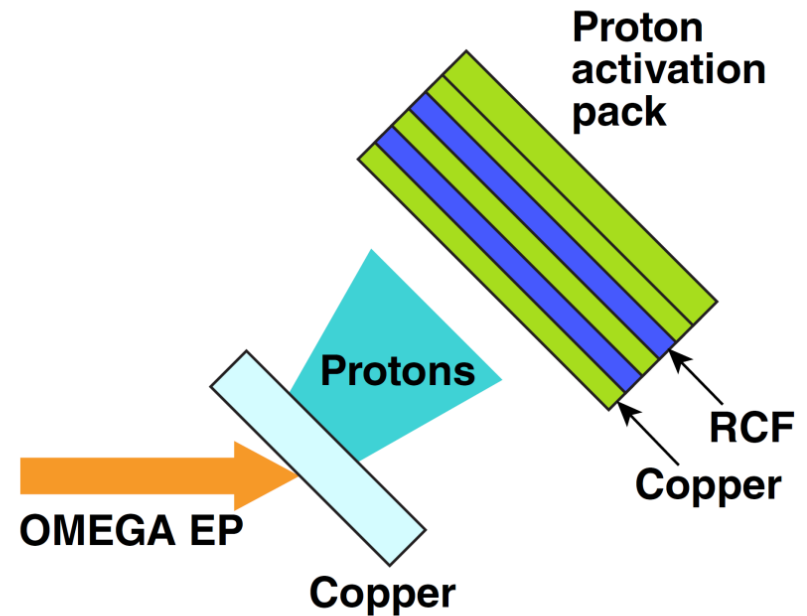




Experiments were performed on OMEGA EP to characterize energetic protons



Focal spot (R_{80})	20 ~ 25 μm
Laser energy	40 J ~ 1500 J
Intensity (average within R_{80})	0.25 ~ 8×10^{18} W/cm²
Intensity contrast	$\sim 10^8$
Targets	500 $\mu\text{m}^2 \times 20 \mu\text{m}$ Cu/Cu+Al/Cu+CH 500 $\mu\text{m}^2 \times 50 \mu\text{m}$ Cu

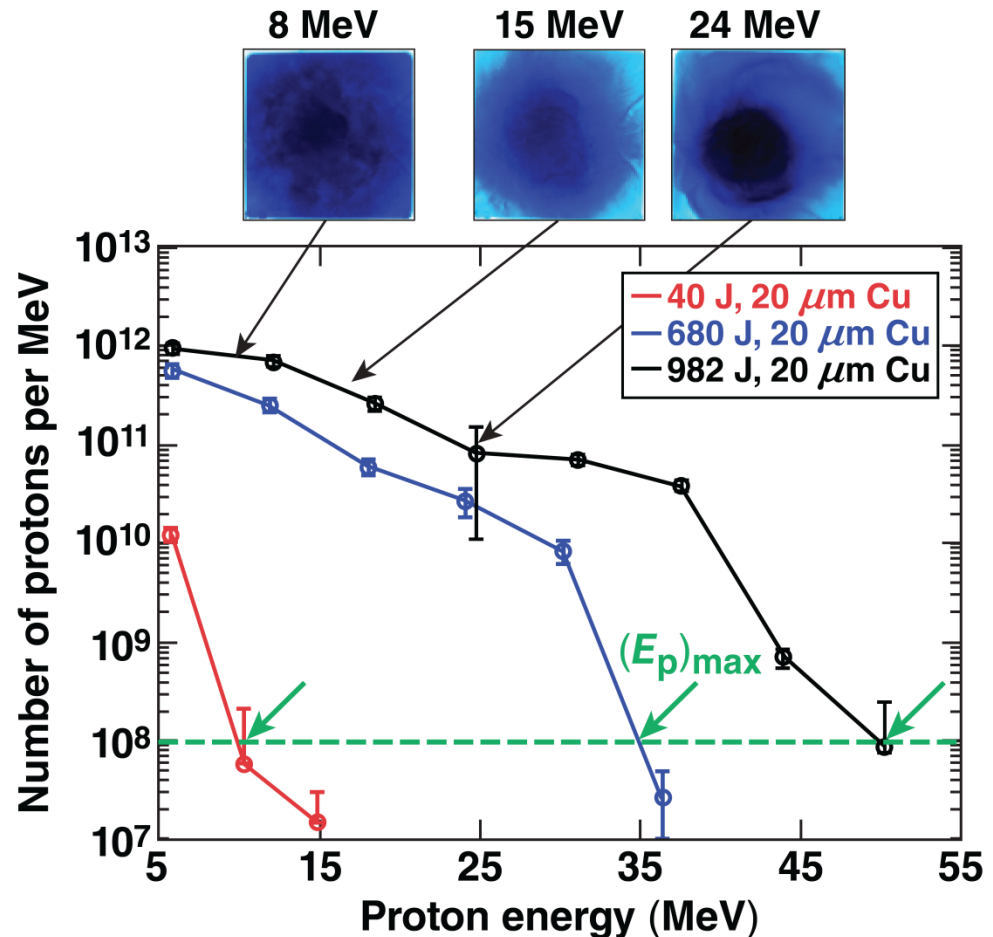




Nuclear activation of copper stacks determined the energy spectrum of the forward-accelerated protons



- Radiochromic film shows proton beam profile
- ^{63}Cu (p, n) ^{63}Zn
 ^{65}Cu (p, 3n) ^{63}Zn
- Coincidence counter absolutely calibrated using known source Na_{22}
- Response functions using stopping power* and cross-section data**
- An iterative method to recover the energy spectrum

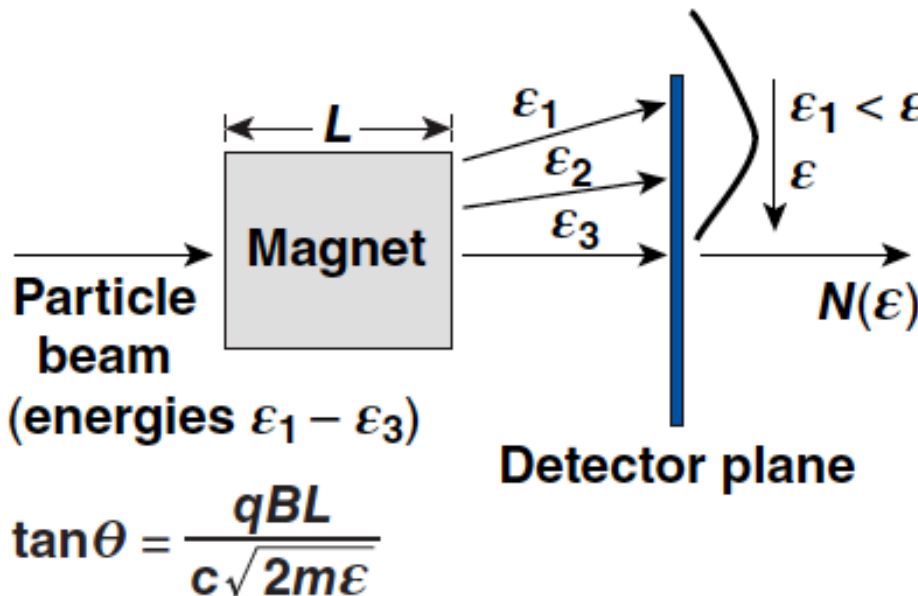


* <http://physics.nist.gov/Star>.

** <http://www.nndc.bnl.gov/exfor/>.



The energy spectrum of high-energy charged particles can be measured with a magnetic spectrometer



- Some issues

- must know the detector response as a function of ε
- $\frac{\Delta\varepsilon}{\varepsilon}$ is smaller at higher energy
- the design can be optimized
 - magnet geometry
 - detector-plane orientation

- A major limitation is that the spectrometer cannot resolve among particles with the same sign of charge but different q, m, ε degenerate

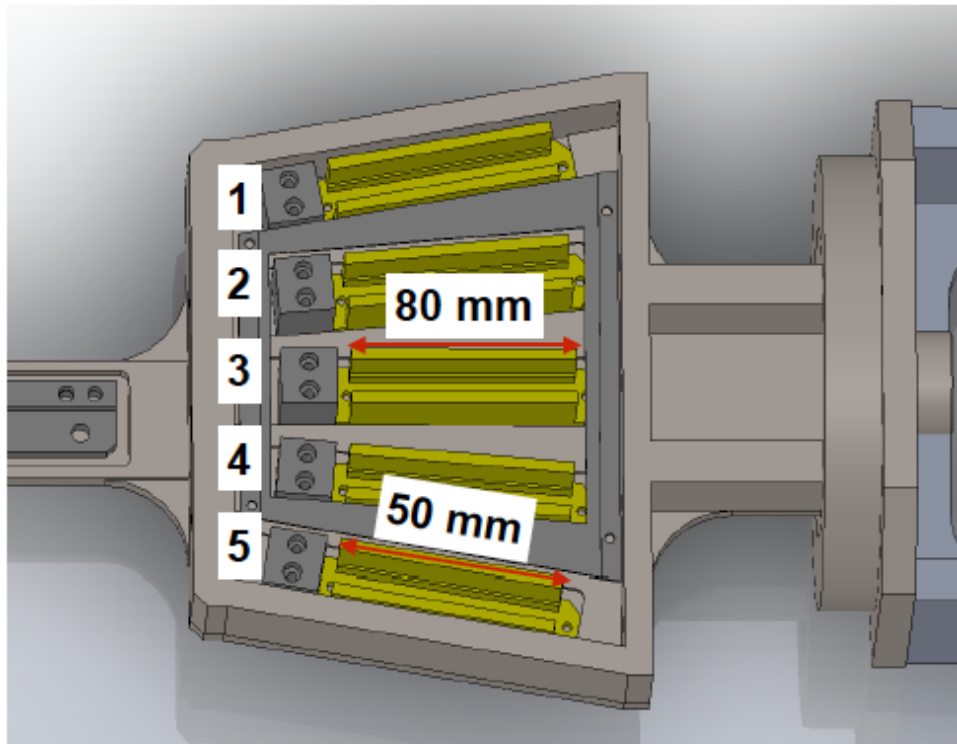
- A magnetic spectrometer works well for
 - electrons, positrons
 - ions when only a single species is present—typically protons



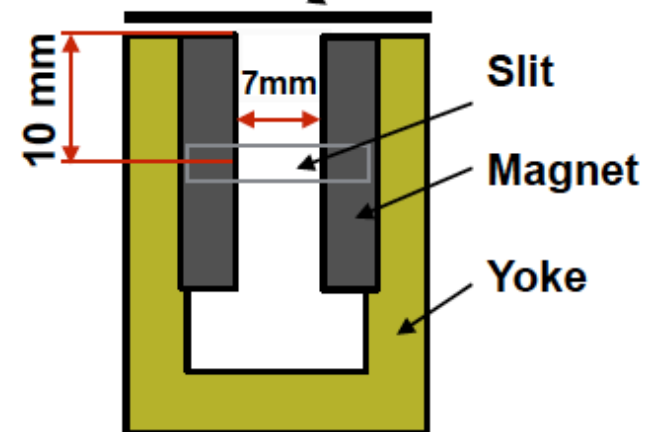
The energy spectrum of high-energy charged particles can be measured with a magnetic spectrometer



OU-ESM



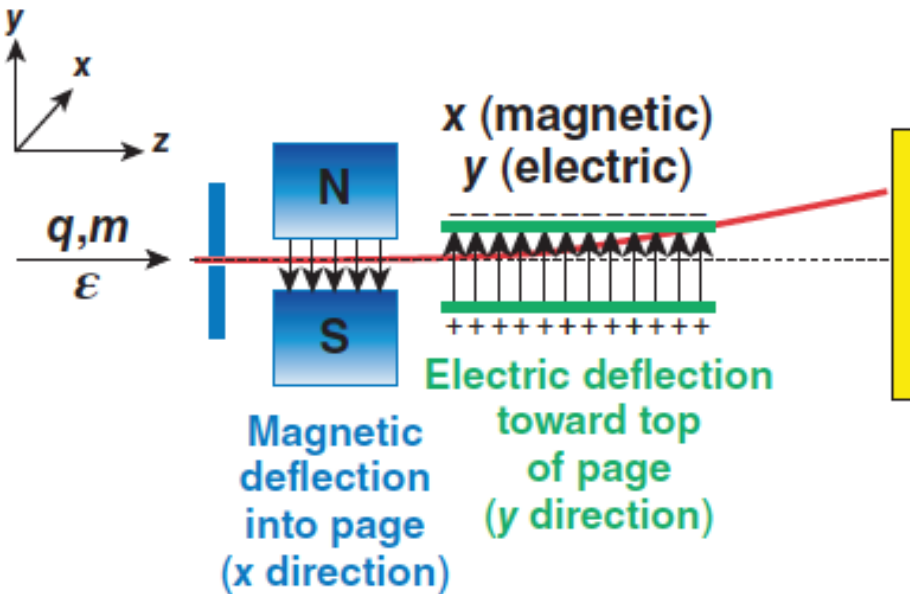
Lid with
IP detector



Ch1 -10°	50 mm length
Ch2 -5°	80 mm length
Ch3 -0°	80 mm length
Ch4 +5°	80 mm length
Ch5 +10°	50 mm length



A Thomson parabola uses parallel electric and magnetic fields to deflect particles onto parabolic curves that resolve q/m



- Deflection caused by magnetic field $\sim q/p$
- Deflection caused by electric field $\sim q/KE$
- Ion traces form parabolic curves on detector plane

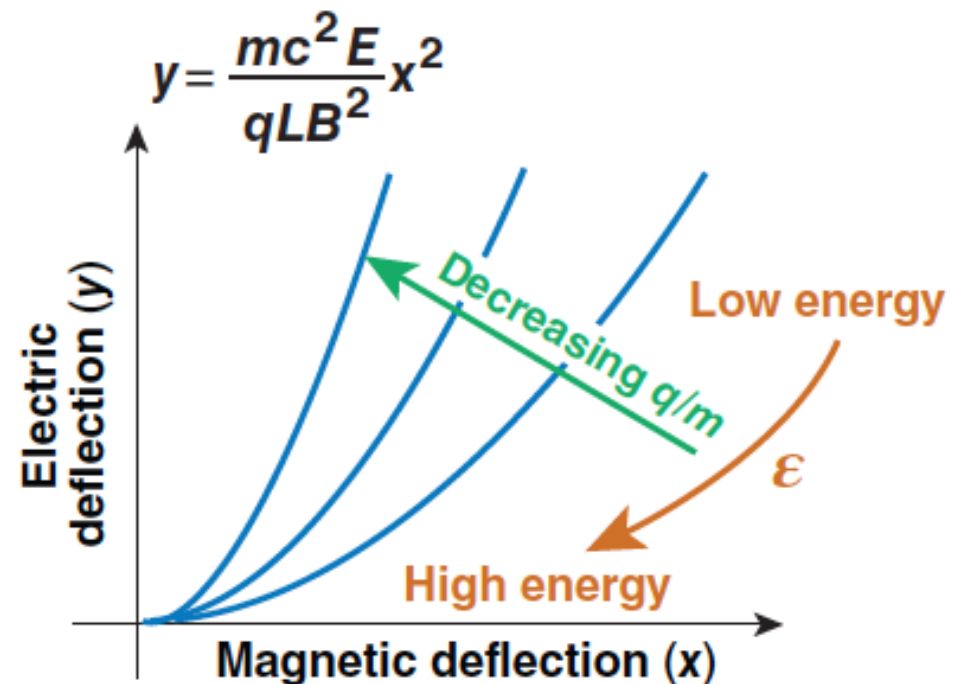
$$\tan \Delta\theta_x = \Delta\theta_x = \frac{qBL}{c\sqrt{2m\epsilon}}$$

y deflection

$$F_{\perp} = qE$$

$$\Delta mV_y = qE\tau = \frac{qEL}{V}$$

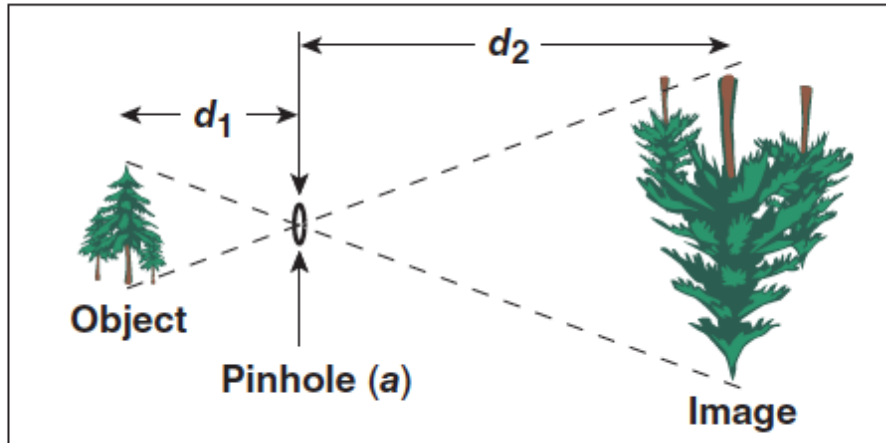
$$\tan \theta_y \sim \theta_y = \frac{\Delta mV_y}{mV} = \frac{qEL}{2\epsilon}$$



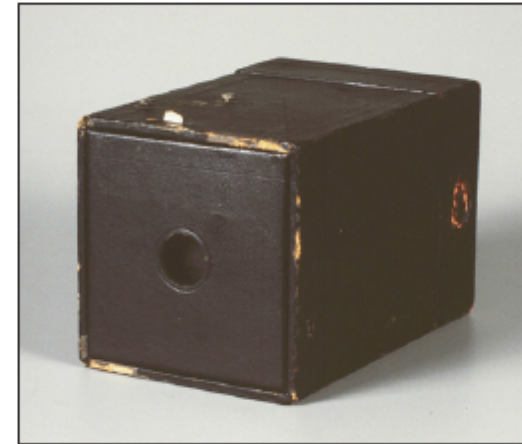
- **Basic diagnostic building blocks**
 - **Electromagnetic field**
 - **Proton radiography**
 - **Particles**
 - **RCF stack / Proton activation pack / Electron spectrometer / Thomson parabola**
 - **X rays**
 - **Pinhole camera (time integrated) / 1-D streak camera / 2-D framing camera**
 - **Plasma conditions**
 - **High-resolution x-ray spectroscopy / Thomson scattering / Neutrons / x-ray radiography**



The simplest imaging device is a pinhole camera



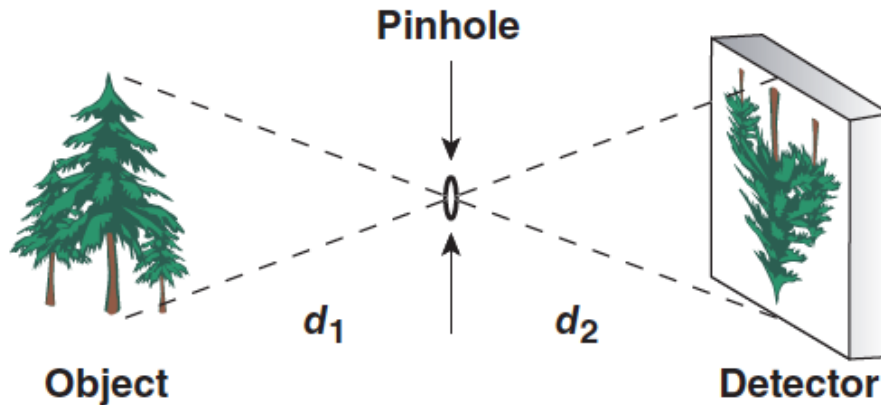
Kodak Brownie camera



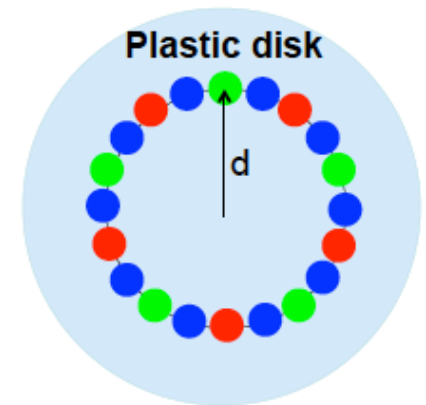
- Magnification = $\frac{d_2}{d_1}$
- Infinite depth of field (variable magnification)
- Pinhole diameter determines
 - resolution $\sim a$
 - light collection: $\Delta\Omega = \frac{\pi}{4} \frac{a^2}{d_1^2}$

Imaging optics (e.g., lenses) can be used for higher resolutions with larger solid angles.

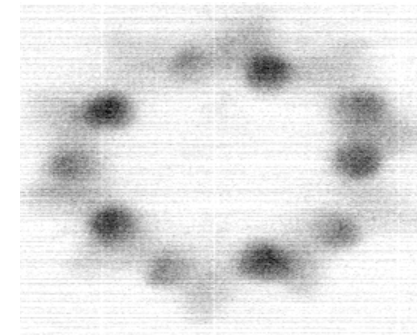
2-D time-integrated images can be recorded on film or electric detectors



Magnetized Jet Exp



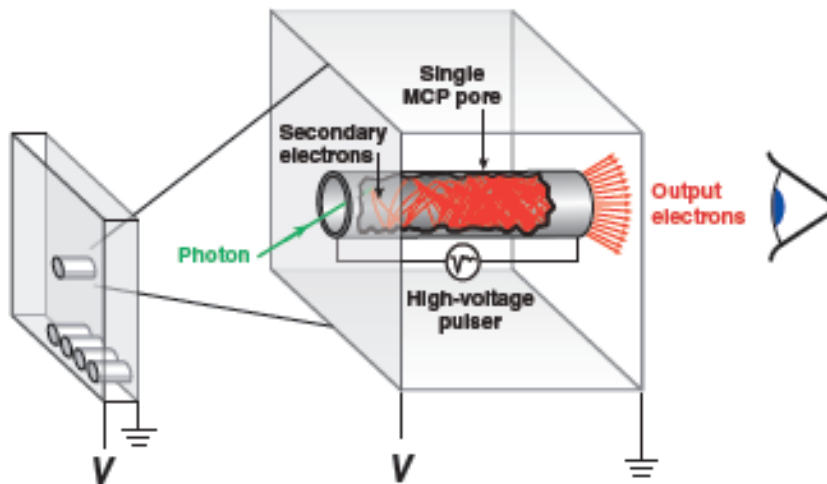
- A 2-D detector is required for a pinhole camera
 - film—requires processing
 - electronic
 - semiconductor arrays—signal proportional to incident flux per pixel (CCD or CID)
 - array of ionization detectors
 - single-photon counters—limited dynamic range



A framing camera provides a series of time-gated 2-D images, similar to a movie camera

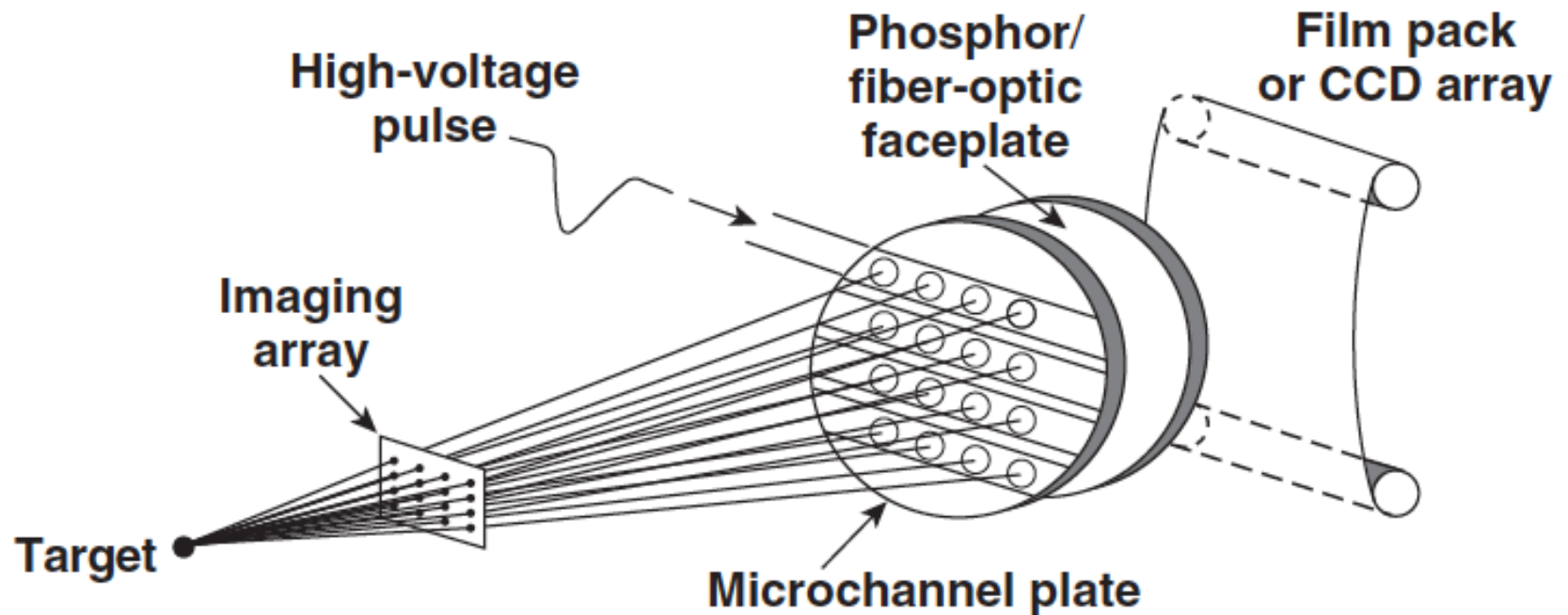


- The building block of a framing camera is a gated microchannel-plate detector (MCP).
- An MCP is a plate covered with small holes.



Multiple electrons are produced each time an electron or photon hits the wall.

Two-dimensional time-resolved images are recorded using x-ray framing camera

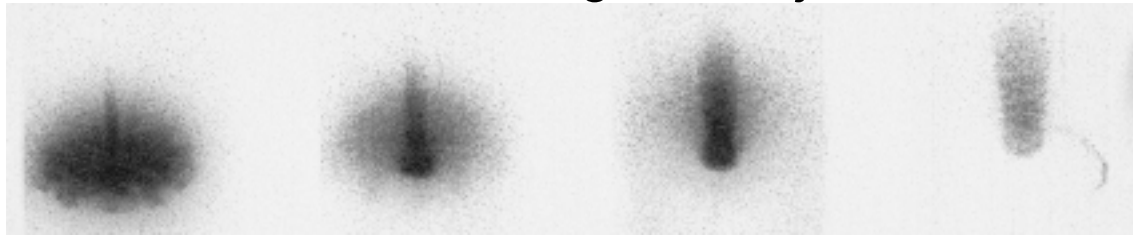


- Temporal resolution = 35 to 40 ps
- Imaging array: Pinholes: 10- to 12- μm resolution, 1 to 4 keV
- Space-resolved x-ray spectra can be obtained by using Bragg crystals and imaging slits

Two-dimensional time-resolved images are recorded using x-ray framing camera

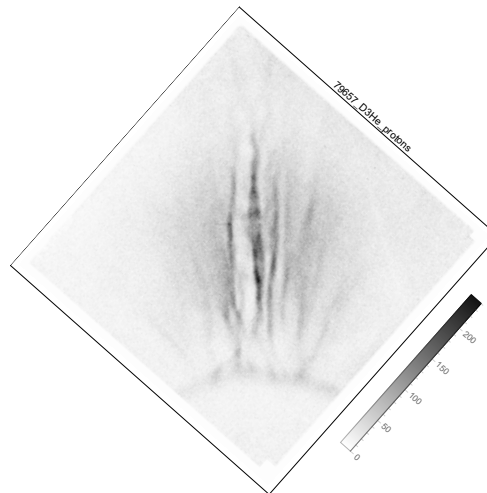


X-ray framing camera: self-emission of the magnetized jet

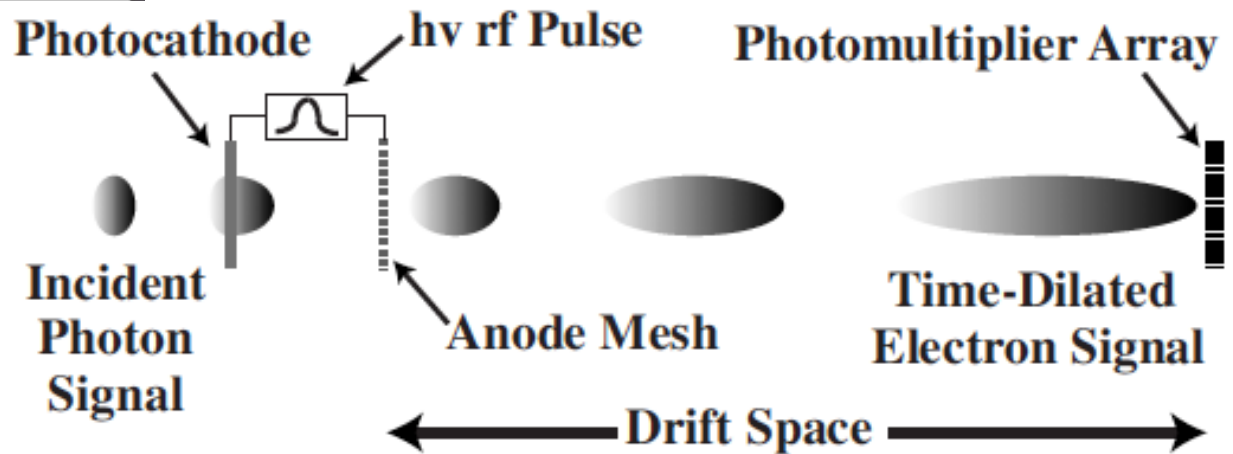
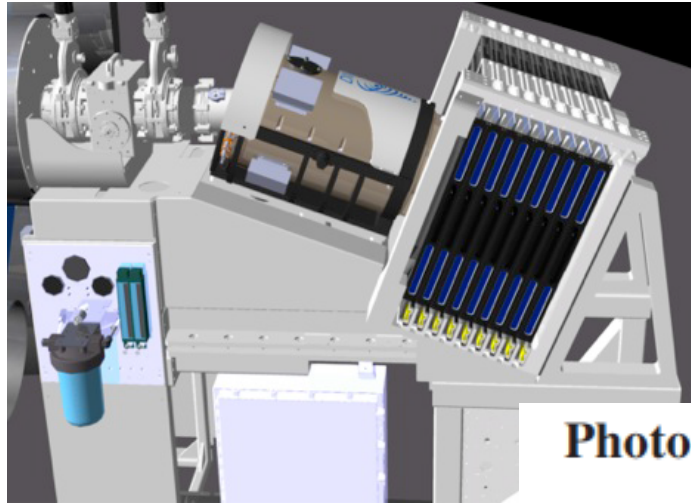


Time

Proton radiography: magnetic fields around the magnetized jet

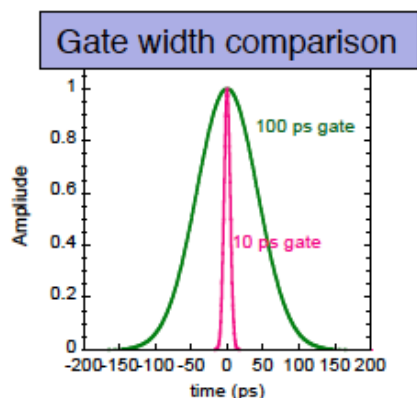
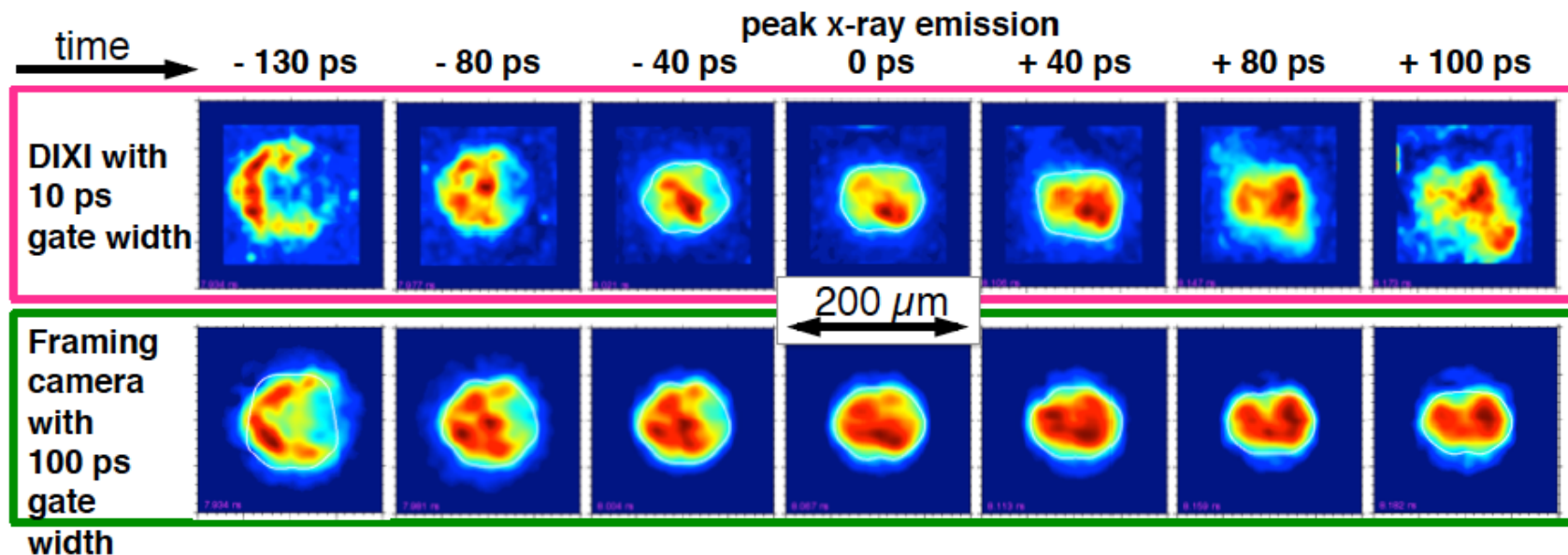


NIF's gated x-ray framing camera DIXI has 10-ps temporal resolution and observes features not seen with NIF's last century gated x-ray cameras



*T. J. Hillsbeck et al., RSI 81, 10E317 (2010)

DIXI takes clearer pictures of the hot spot evolution around peak x-ray emission



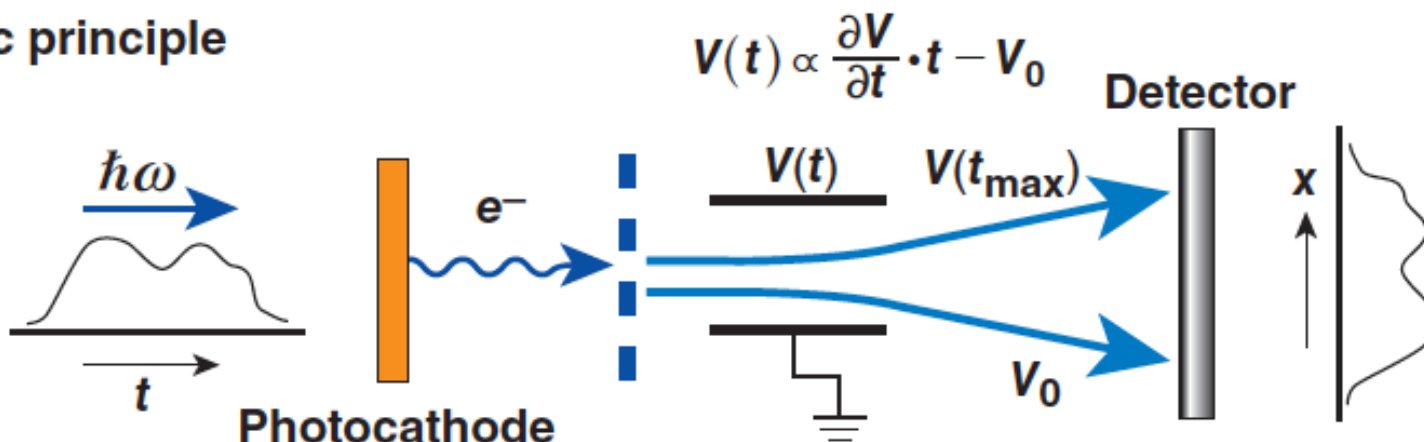
DIXI's 10X higher temporal resolution (reduced temporal blur) reveals details in the evolution of implosions at NIF never before possible, using the slower cameras.

N141116

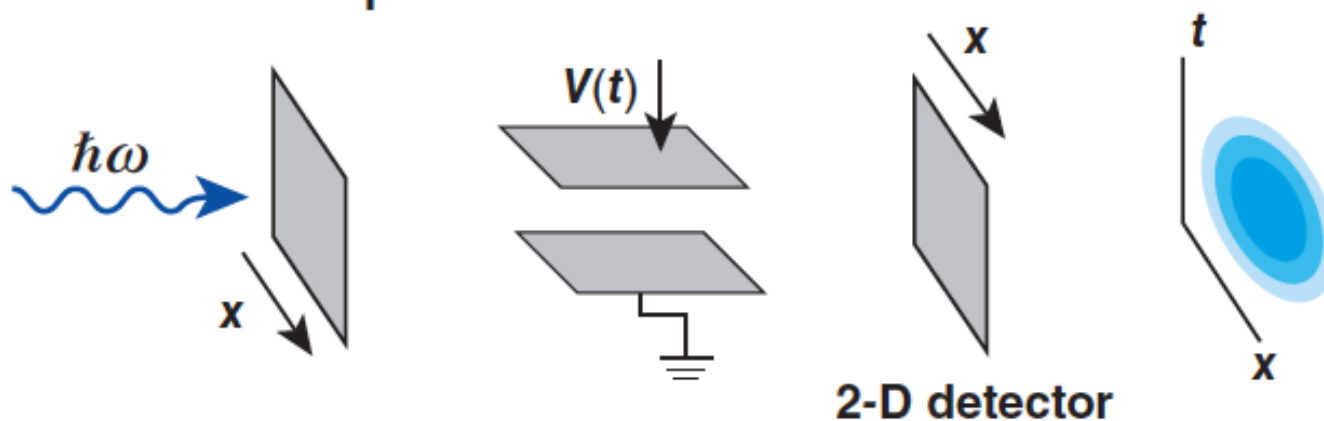
A streak camera provides temporal resolution of 1-D data



Basic principle

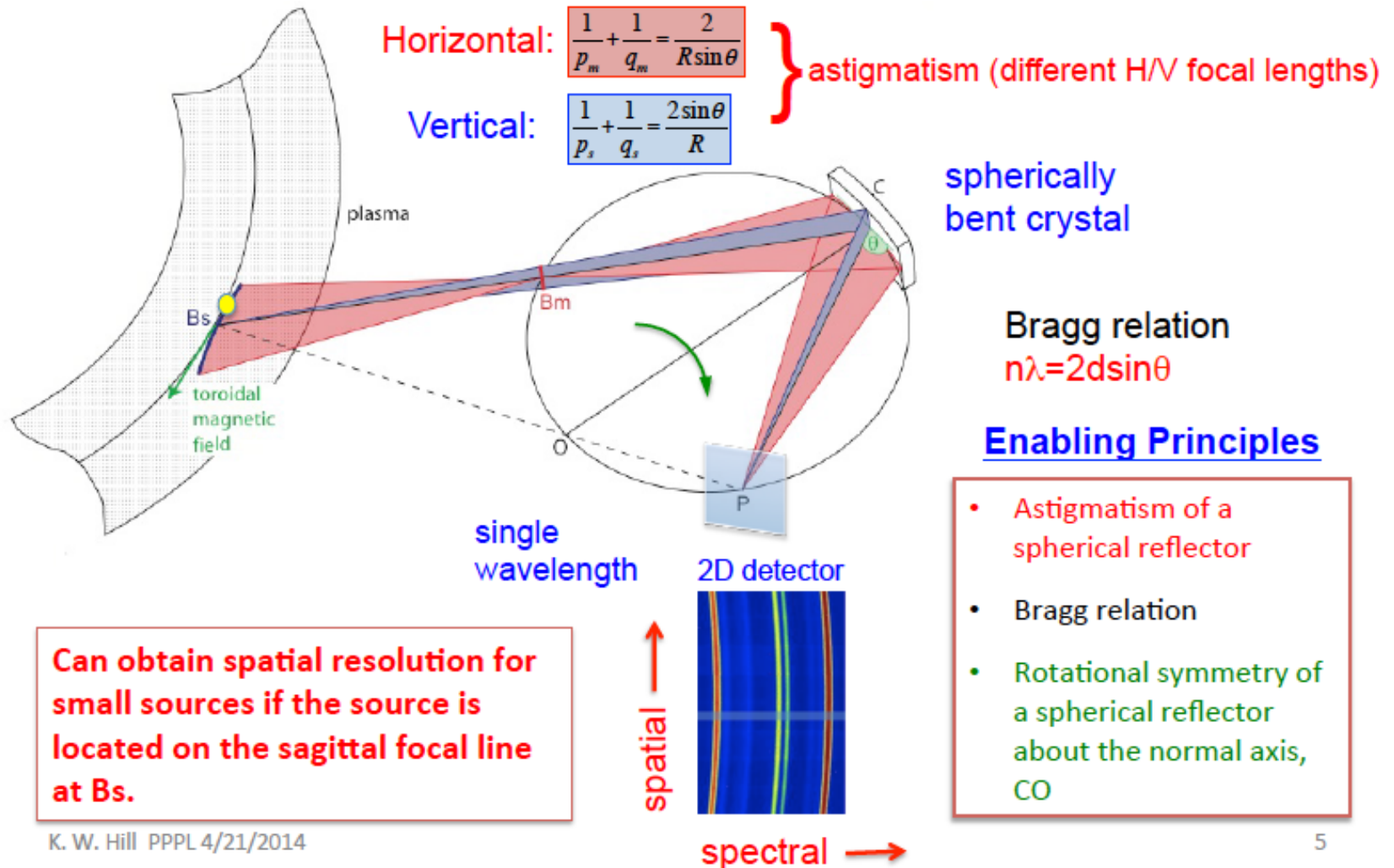


A streak camera can provide 2-D information



- **Basic diagnostic building blocks**
 - **Electromagnetic field**
 - **Proton radiography**
 - **Particles**
 - **RCF stack / Proton activation pack / Electron spectrometer / Thomson parabola**
 - **X rays**
 - **Pinhole camera (time integrated) / 1-D streak camera / 2-D framing camera**
 - **Plasma conditions**
 - **High-resolution x-ray spectroscopy / Thomson scattering / Neutrons / x-ray radiography**

High-resolution x-ray spectroscopy is well-established on Tokamaks for measuring plasma conditions



High-resolution x-ray spectroscopy is well-established on Tokamaks for measuring plasma conditions



X-ray Crystal Spectrometer Makes Debut at C-Mod

New Technique a Major Advance for ITER

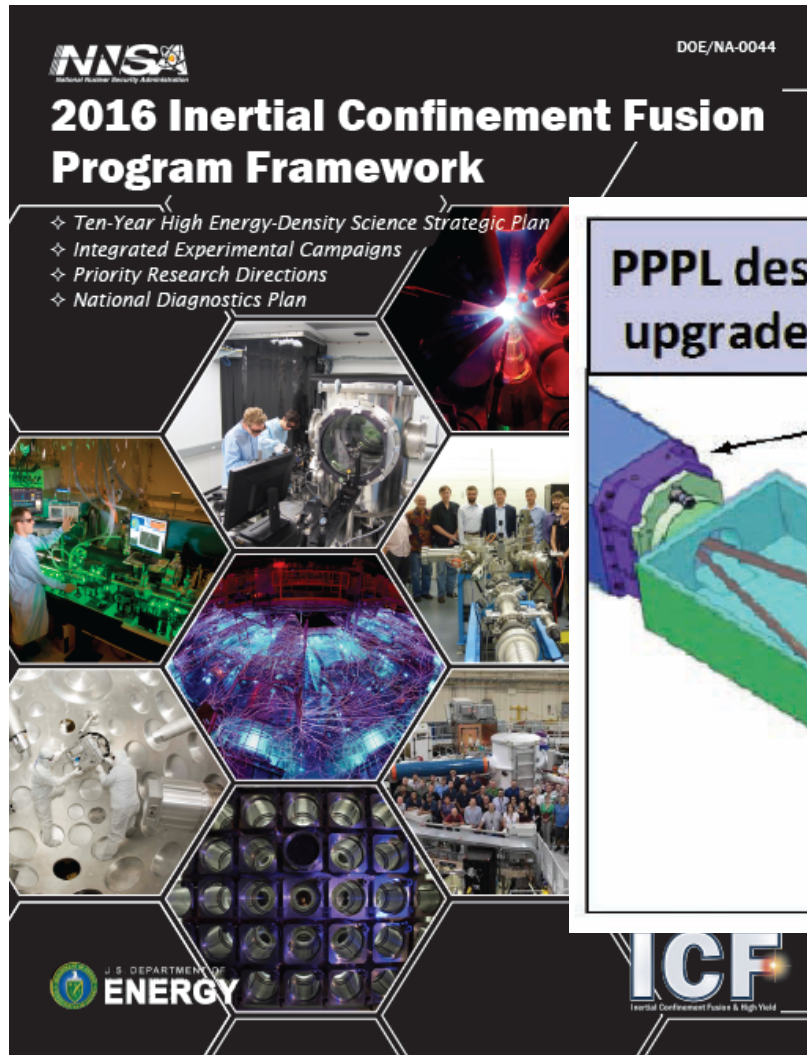
A PPPL/Alcator C-Mod collaboration has resulted in the demonstration of a greatly improved X-ray crystal spectrometer for application to ITER and fusion reactors. Experiments conducted by a PPPL/MIT team in April mark the beginning of a new era in the ability of such devices to determine radial profiles of the ion temperature and the rotational velocity of high temperature plasmas without the need for diagnostic beams. Their success will benefit substantially ITER and other advanced fusion energy systems.



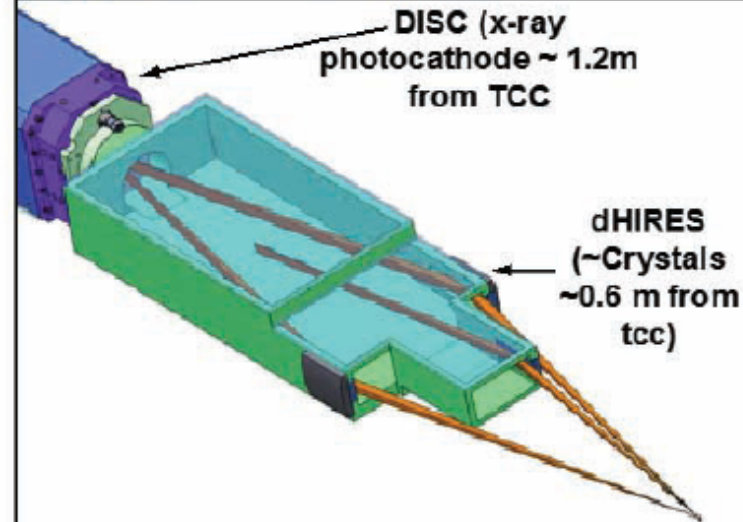
From the left are: Alex Ince-Cushman, MIT; Ken Hill, PPPL; Manfred Bitter, PPPL; John Rice, MIT; and Christian Broennimann of the Paul Scherrer Institute in Switzerland.

impurity by the pattern of frequencies, or spectrum, of the light emitted and they can determine the

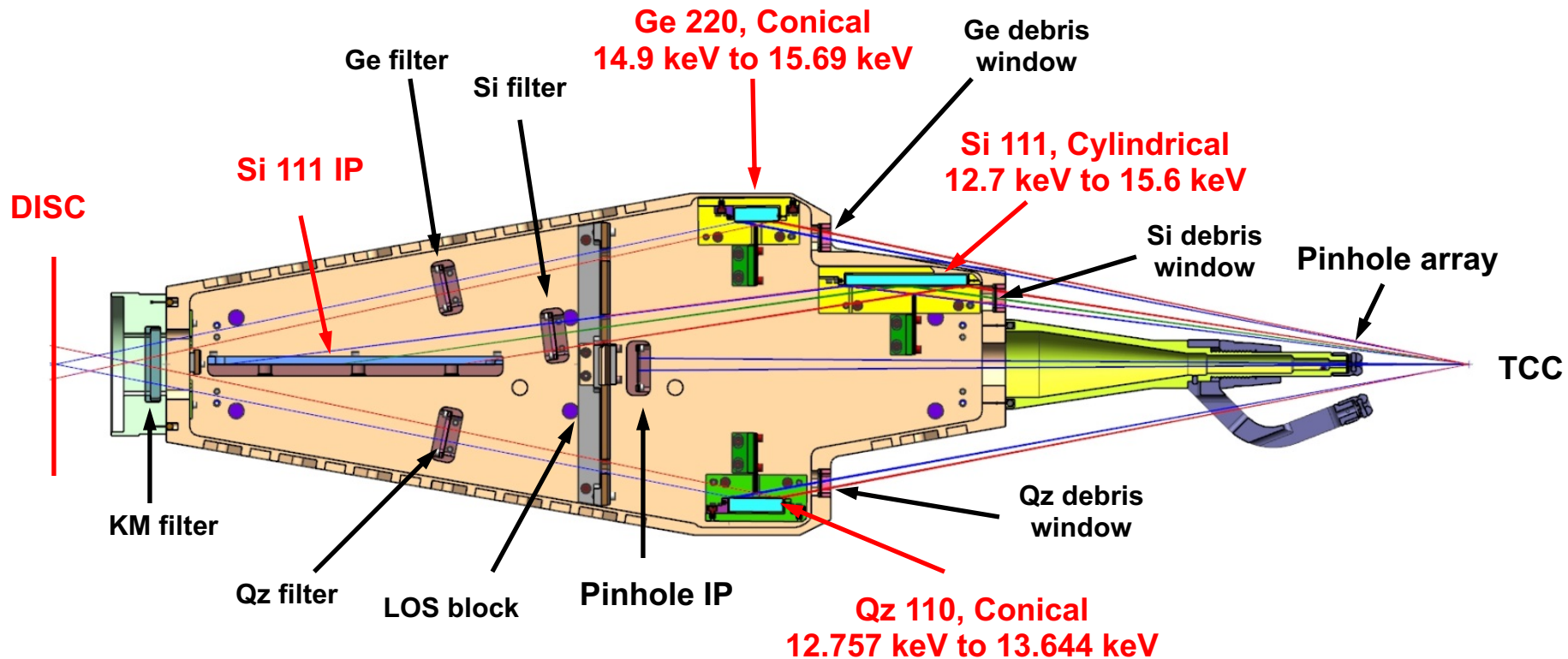
PPPL designed high-resolution x-ray spectrometer has been identified as one of the 8 National Transformative Diagnostics



PPPL designed, LLE built spect,
upgraded x-ray streak camera



DHIRES contains three spectrometer channels and one imaging channel

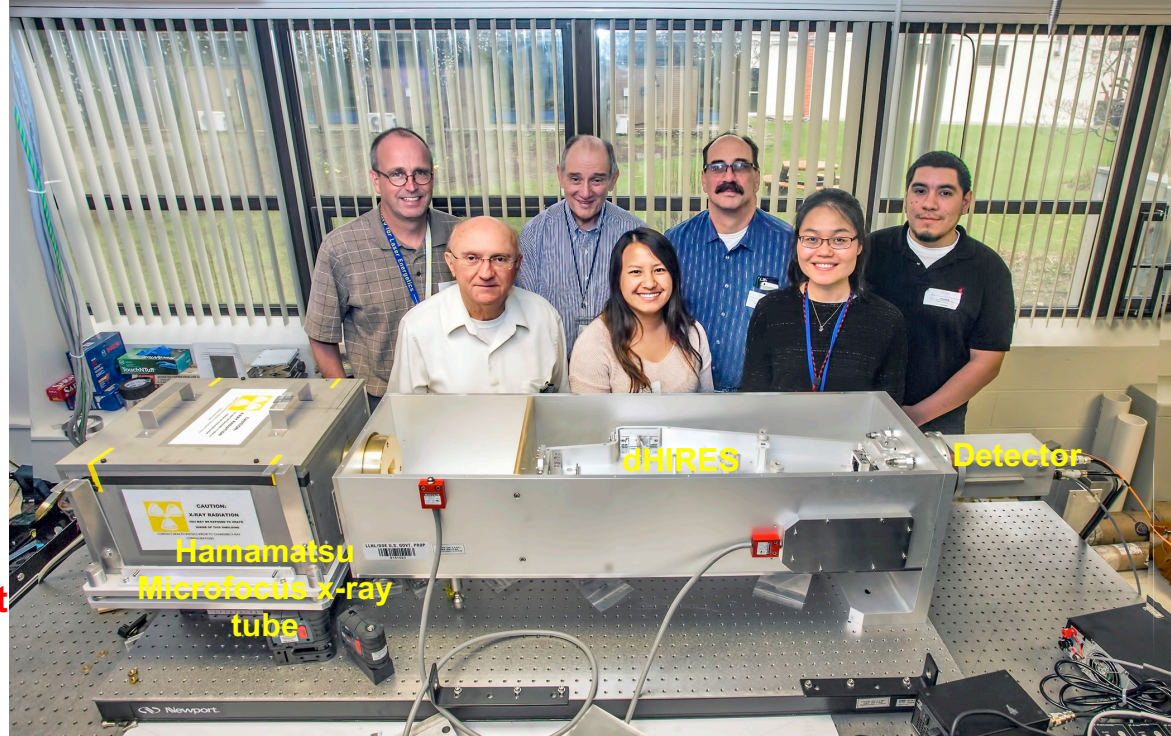


T. Hall geometry: J.Phys. E. 17, 110 (1984)

DHIRES is fully calibrated at the PPPL x-ray lab*



- Source Alignment
- Crystal Evaluation
- Energy Calibration and Crystal Dispersion
- Spectrum Manipulation
- Source Displacement and Insertion Error
- Absolute Throughput Measurement and NIF Signal Level Prediction
- Optical Alignment



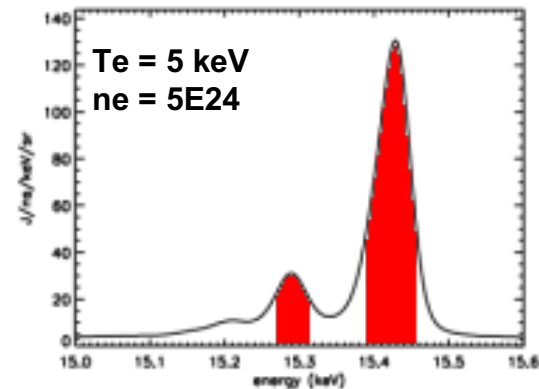
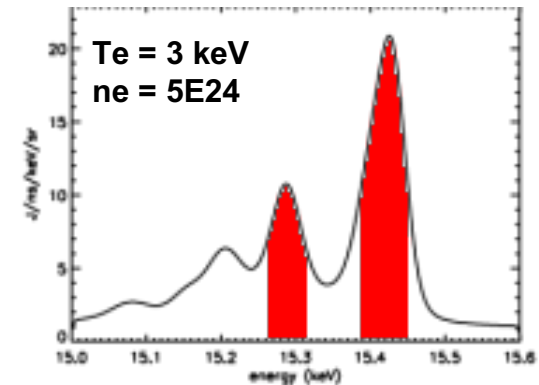
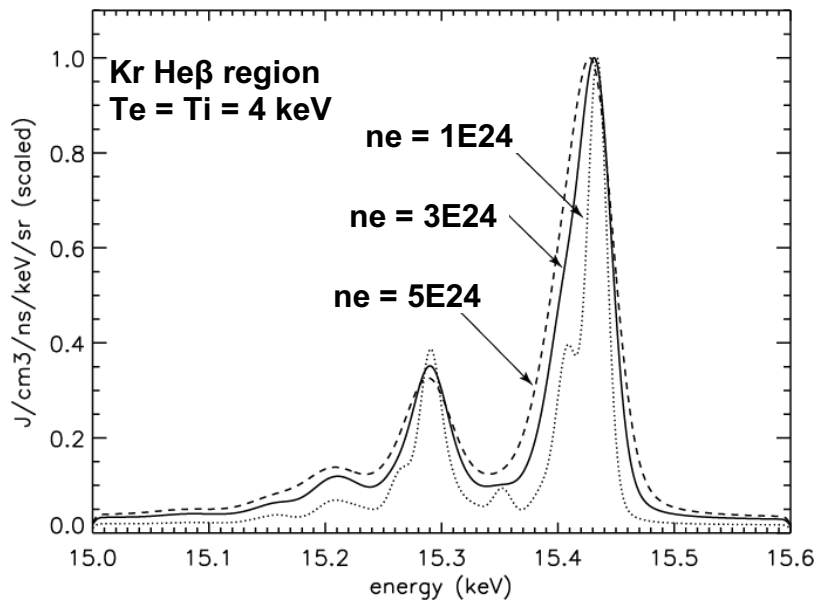
The spectral resolution is ~10 eV

*L. Gao et al., RSI **89**, 10F125 (2018)

Stark broadening of Kr He β measures n_e and ratio of He-like resonance line to Li-like satellite provides T_e



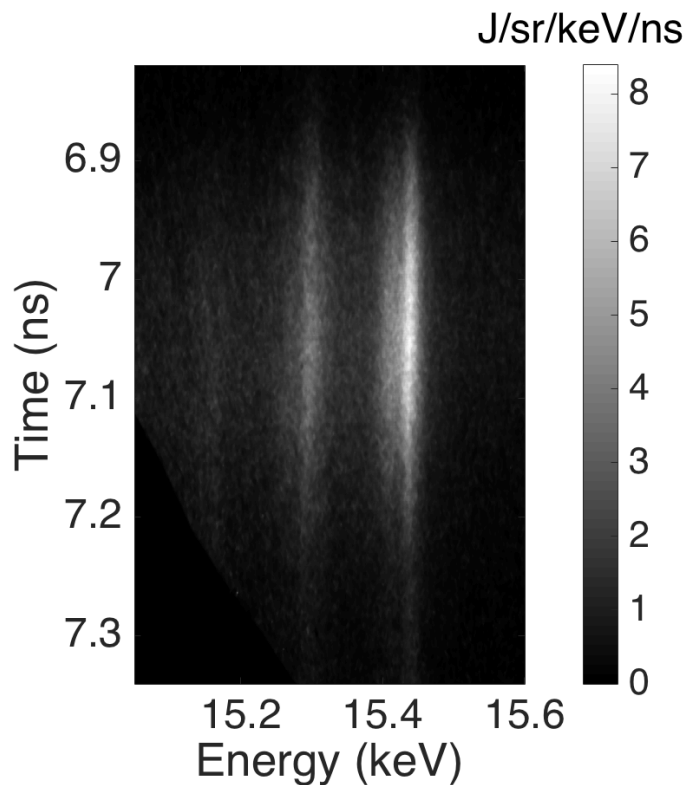
SCRAM calculation for a SymCap implosion Cr: D. Liedahl



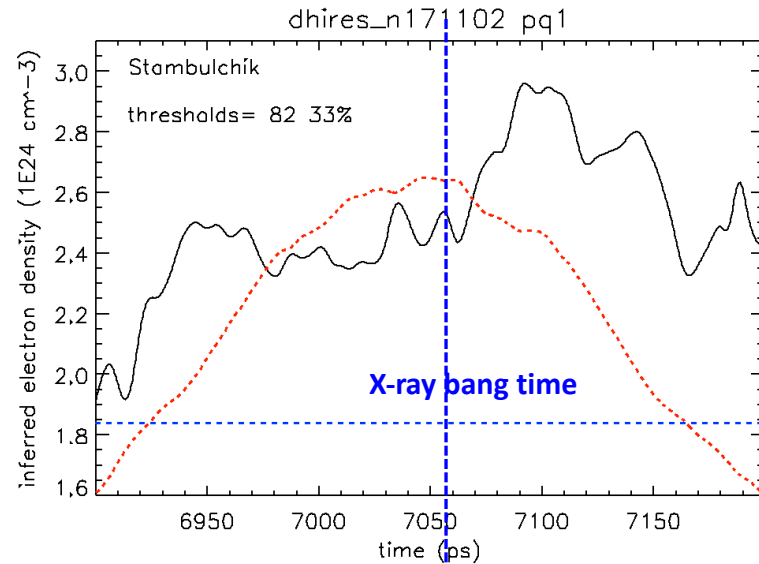
Stark broadening of Kr He β measures n_e and ratio of He-like resonance line to Li-like satellite provides T_e



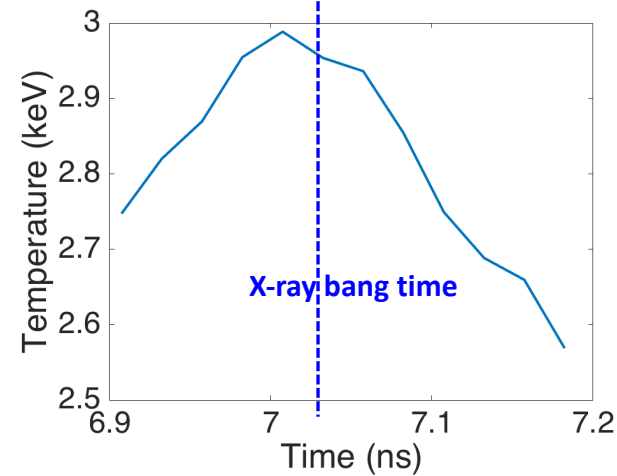
Calibrated DISC, He β
NIF N171102-003



Inferred $n_e(t)$ by comparing Stark width*



Inferred $T_e(t)$

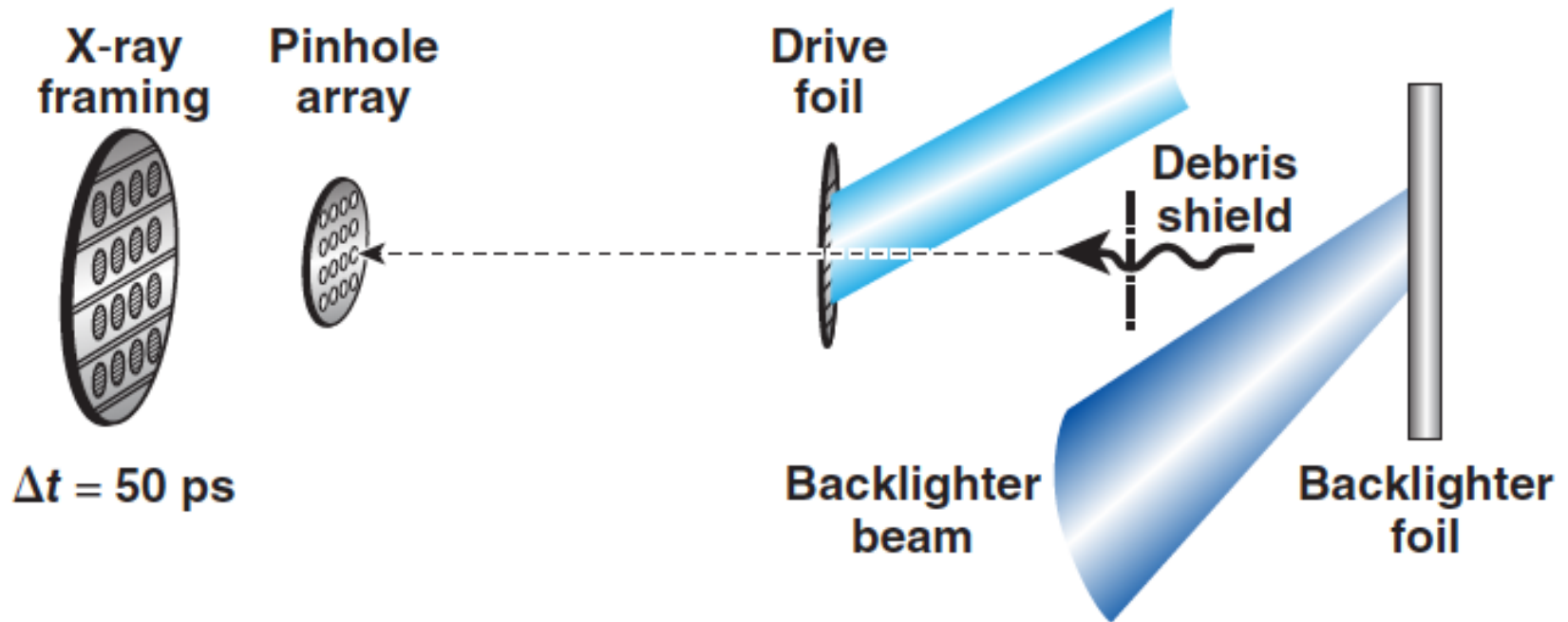




X-ray radiography, coupled with x-ray framing camera, is used to radiograph instability growth



- The backlighter transmission depends on wavelength and target optical depth; mass perturbations lead to optical-depth perturbations



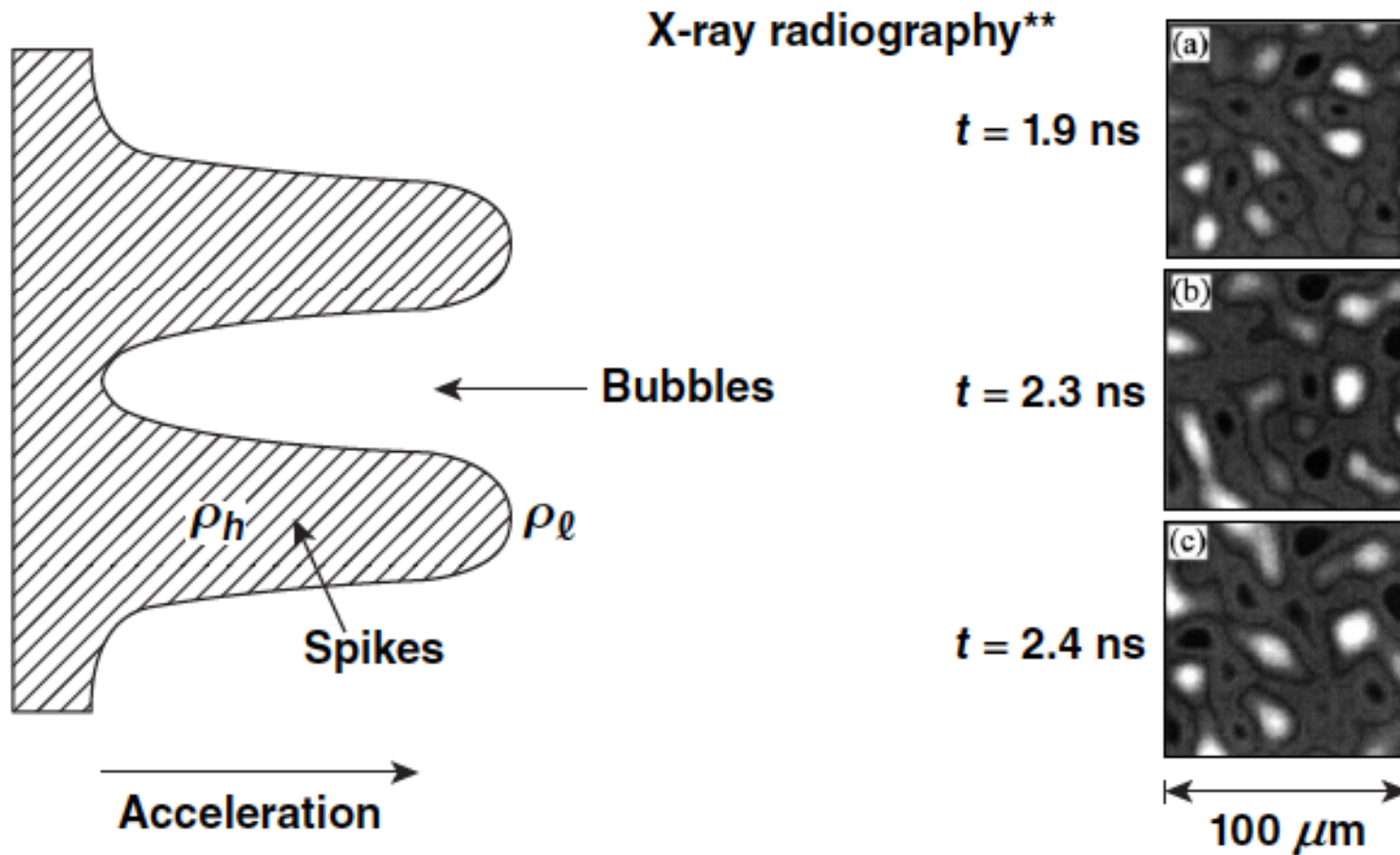
Framing cameras

Spatial resolution
Spatial field of view
Temporal resolution
Temporal field

8 to 10 μm (two dimensions)
500 μm (magnification = 12)
30 to 80 ps
(four) 300-ps strips



A bubble merger is predicted in the nonlinear phase of the RT instability*

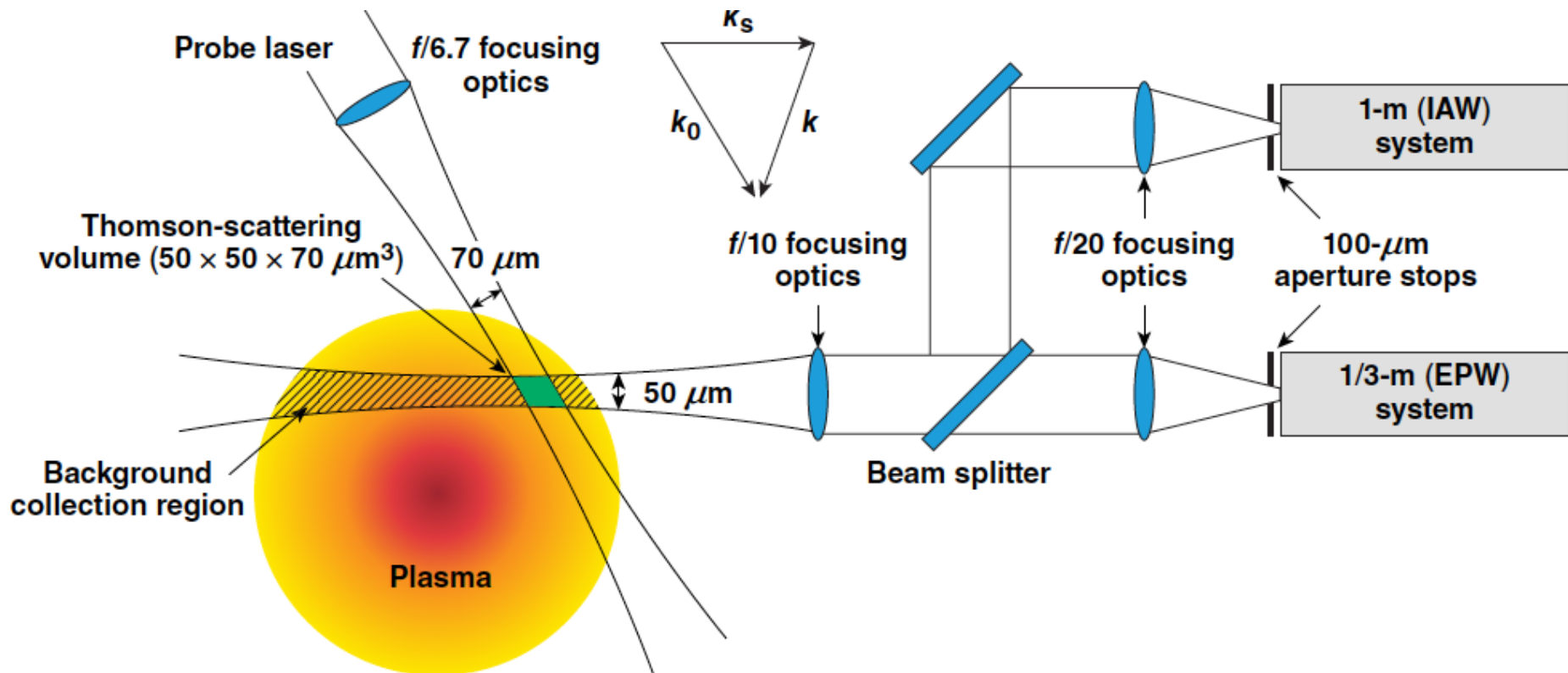


X-ray photons are sensitive to density modulations.

*D. Oron *et al.*, Phys. Plasmas **8**, 2883 (2001);
U. Alon *et al.*, Phys. Rev. Lett. **72**, 2867 (1994).

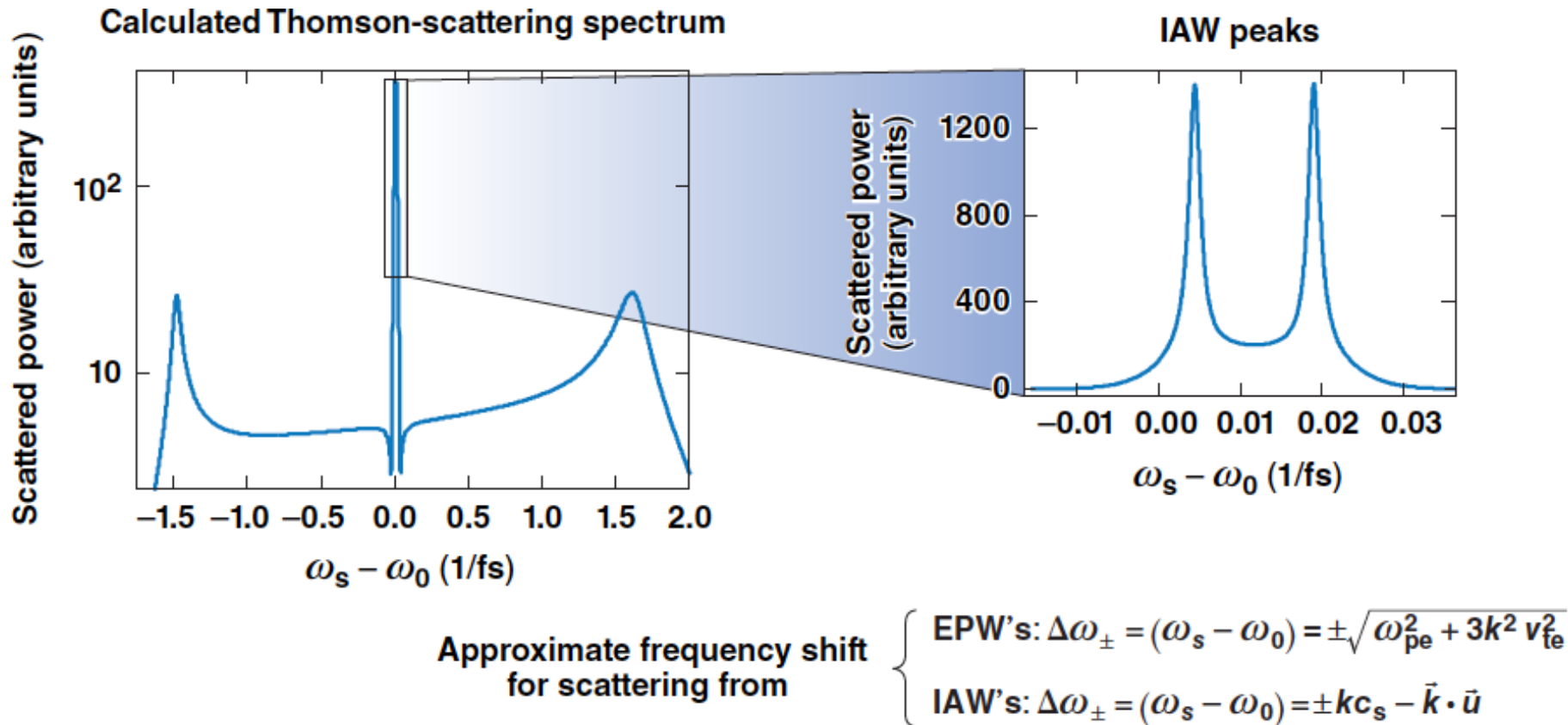
V. A. Smalyuk *et al.*, Phys. Rev. Lett. **81, 5342 (1998).

Optical Thomson scattering is used to diagnose local plasma conditions by observing the spectrum of light scattered from a probe beam over a small interaction volume



*R. Follet et al, RSI 87, 11E401 (2016)

Plasma parameters are inferred by comparing measured Thomson-scattering spectra to calculated spectra



Electron density and temperature, ion temperature, and flow velocity were measured inside the magnetized jet



OMEGA beams:

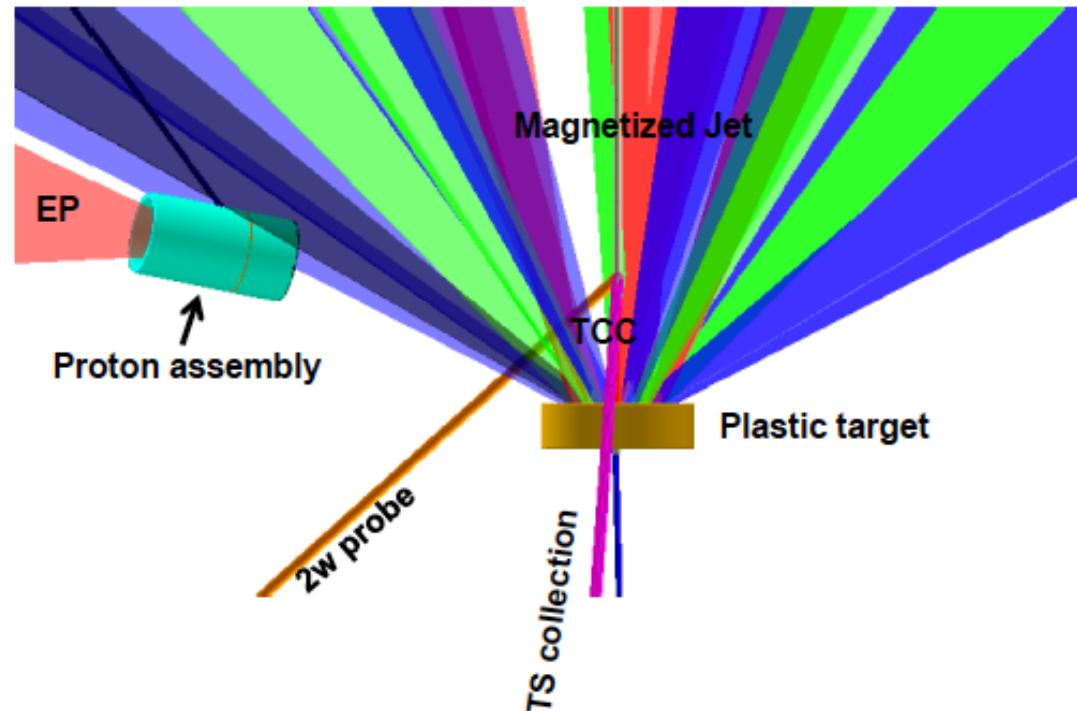
- Ring 1: 17, 22, 46, 56, 61
- Ring 2: 11, 26, 31, 55, 68
- Ring 3: 10, 13, 20, 28, 33, 48, 52, 58, 65, 66

OMEGA EP BL:

- Maximum energy, 10 ps (may switch to 1 ps)
- Best focus
- 8 mm from TCC toward H7

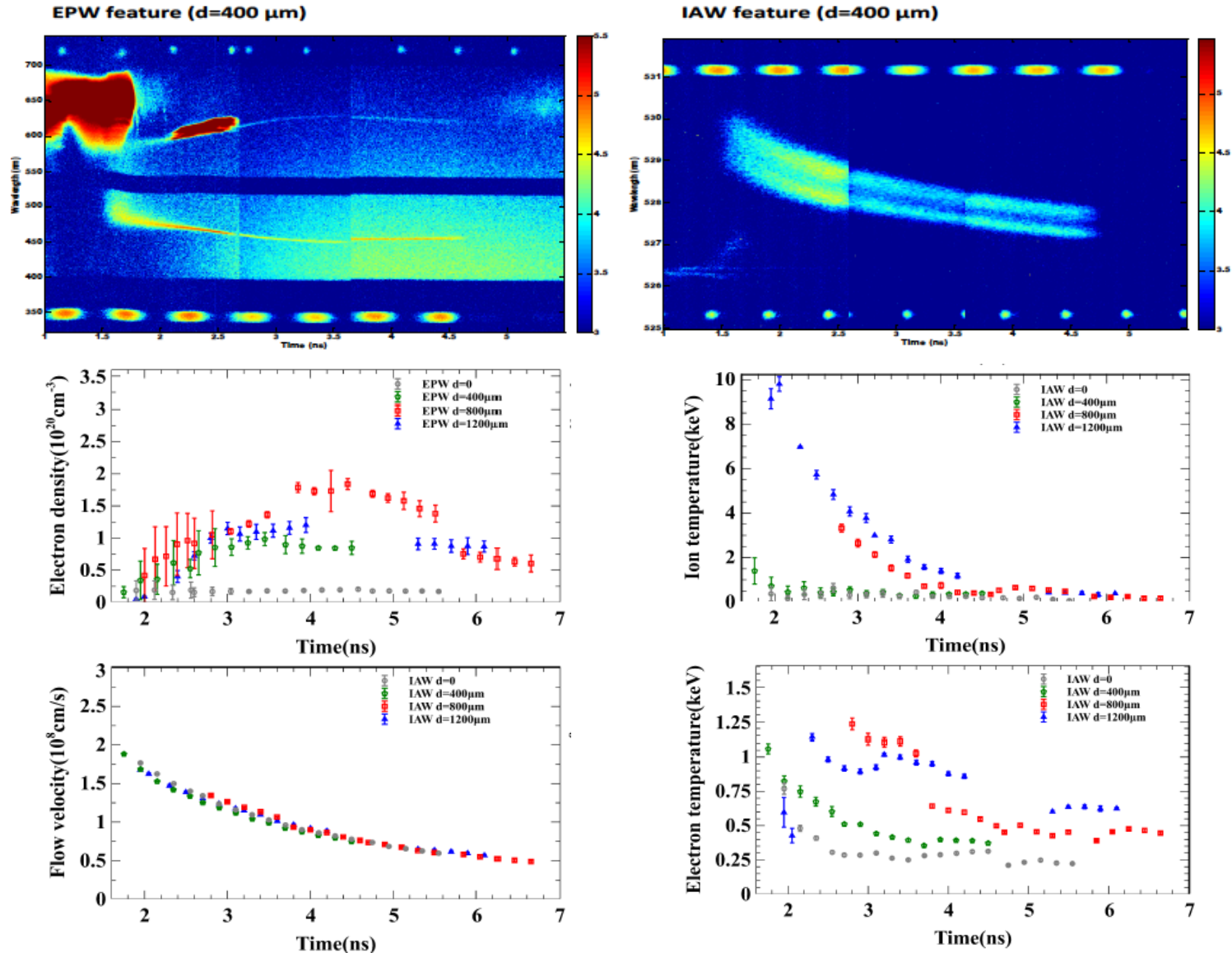
Diagnostics:

- TIM 5: Titled CPRM as the proton detector
Distance is 16.5 cm from TCC
- TIM 6: TS collection system
- TIM 3: TTPS for the main plastic target
- **TIM 4: XRFC (changed from TIM 2 to TIM 4)**
- H2: EP proton generation assembly target stalk



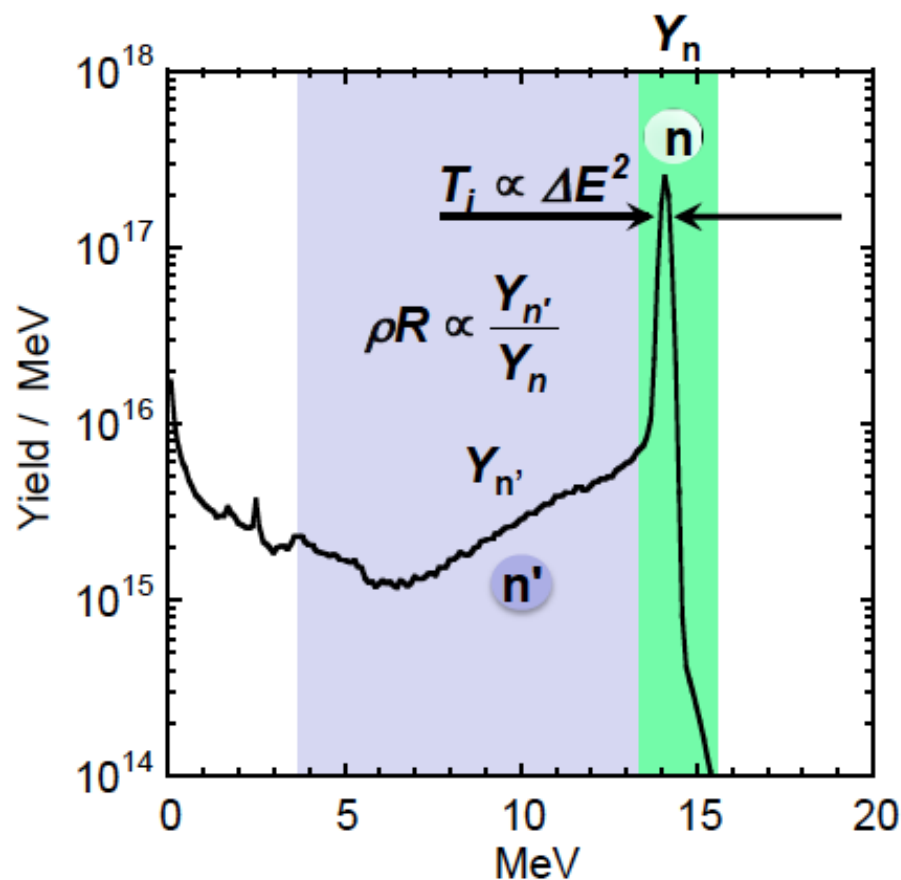
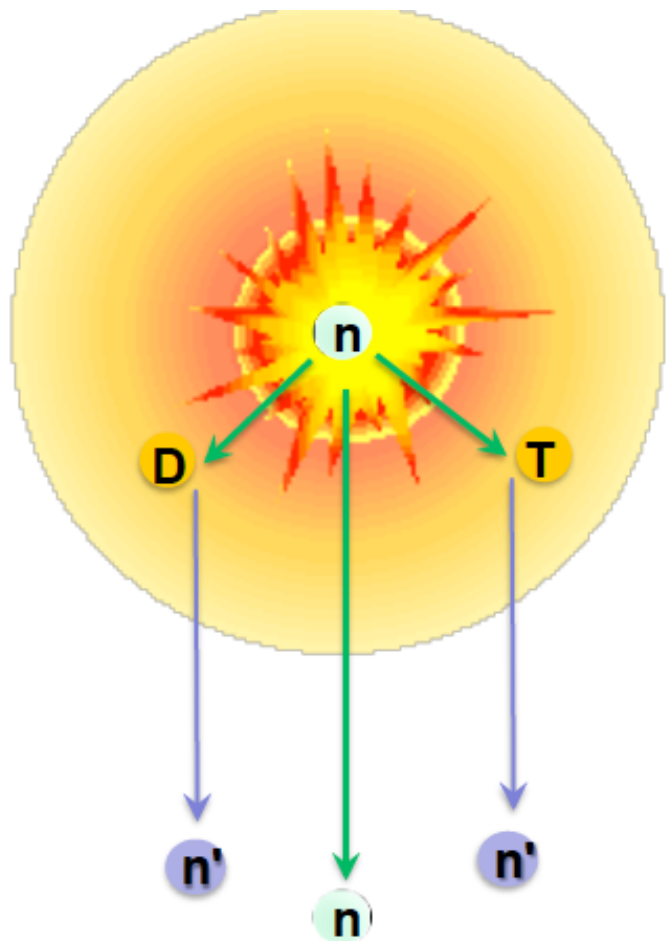


Electron density and temperature, ion temperature, and flow velocity were measured inside the magnetized jet





The neutron spectrum provides information on ρR , Ti and yield – essential for assessing the implosion performance



A large suite of diagnostics have been developed for HEDP facilities



- **HEDP systems generate some or all of**
 - Visible light
 - UV and x-ray photons
 - Charged particles
 - Neutrons
 - Strong fields
- **A comprehensive diagnostic suite makes it possible to learn a great deal about the systems: field strength and their impact, plasma parameters (n_e , n_i , T_e , v), particles, instabilities, yield, etc...**
- **Diagnosing HED systems require very high temporal (sub-ns, ps) and spatial ($\sim 10 \mu\text{m}$) resolution**
- **Advances in technology and diagnostics enable understanding of new physics**